

# For Reference

---

NOT TO BE TAKEN FROM THIS ROOM

# For Reference

---

NOT TO BE TAKEN FROM THIS ROOM

Ex LIBRIS  
UNIVERSITATIS  
ALBERTAE







Digitized by the Internet Archive  
in 2019 with funding from  
University of Alberta Libraries

<https://archive.org/details/Tso1963>

THE UNIVERSITY OF ALBERTA

A STUDY OF LATERALLY LOADED THIN FLAT PLATES

BY THE MOIRE METHOD

A THESIS

SUBMITTED TO THE FACULTY OF GRADUATE STUDIES

IN PARTIAL FULFILMENT OF THE REQUIREMENTS FOR THE DEGREE OF

MASTER OF SCIENCE

DEPARTMENT OF MECHANICAL ENGINEERING

by

HONG YEE TSO, B.Sc. (Taiwan)

EDMONTON, ALBERTA

AUGUST, 1963



UNIVERSITY OF ALBERTA  
FACULTY OF GRADUATE STUDIES

The undersigned certify that they have read, and recommend to the Faculty of Graduate Studies for acceptance, a thesis entitled " A Study of Laterally Loaded Thin Flat Plates by the Moir  Method " submitted by Hong Yee Tso in partial fulfilment of the requirements for the degree of Master of Science.



#### ACKNOWLEDGEMENTS

The writer wishes to express appreciation to Dr. K. C. Cheng for his advice and encouragement throughout the work; to Dr. G. Ford for his guidance and interest during the graduate studies at the University of Alberta, and to Mr. D. G. Bellow for his helpful comments and criticisms concerning the manuscript.

He also wishes to thank the staff of the Machine Shop of Mechanical Engineering for their ready assistance.

Funds for the experimental work were provided by the Department of Mechanical Engineering and General Research Grant No. 417.



## ABSTRACT

The feasibility and accuracy of the Moiré method for determining moments and deflections for laterally loaded thin flat plates using Perspex models have been well established by Ligtenberg and Bradley. Metal models are known to have some advantages. In this study, the Moiré method was applied to metal models, e.g. brass and aluminum.

Three cases of bending problems were studied: 1. simply supported square plate with concentrated centre load, 2. clamped square plate with concentrated centre load, and 3. cantilever plate with concentrated load at the midpoint of the free edge opposite to the clamped edge. Theoretical solutions are available for the first two cases and the experimental results by the Moiré method were compared with those obtained by the well known exact solutions. But an exact solution is not available for the last case, and the results from finite difference solution were taken for the comparison.

It is concluded that the metal models are applicable for the Moiré method. This method provides the approximate solutions for the laterally loaded thin flat plate problems which are intractable by analytical methods.



## TABLE OF CONTENTS

	Page
ACKNOWLEDGEMENTS	
ABSTRACT	
LIST OF ILLUSTRATIONS	
LIST OF TABLES	
NOTATIONS	
 CHAPTER	
I      INTRODUCTION.....	1
II     THEORETICAL ANALYSIS.....	4
1. Plate Theory	
2. Boundary conditions	
Simply supported square plate	
Clamped square plate	
Cantilever plate	
III    EXPERIMENTAL INVESTIGATION.....	14
1. The Moire method	
2. Apparatus	
The grid	
The camera	
Model support	
Loading mechanism	
The model	
3. Calibration of the material	
4. Test procedure	
5. Reduction of data	
Preparation of the picture	
Drawing the slope curves	
Determination of curvatures	
Determination of moments	
IV    COMPARISONS OF EXPERIMENTAL RESULTS WITH ANALYTICAL RESULTS.....	43
1. Test results	
Simply supported square plate	
Clamped square plate	
Cantilever plate	
2. Comparisons of the results	
Simply supported square plate	
Clamped square plate	
Cantilever plate	
V     DISCUSSIONS AND CONCLUSIONS.....	54
APPENDIX. COMPUTER PROGRAMS AND DATA.....	58
1. Simply supported square plate	
2. Clamped square plate	
BIBLIOGRAPHY.....	71



## LIST OF ILLUSTRATIONS

Figure	Page
1. The element of a plate.....	5
2. Simply supported square plate with load $P$ at the centre.....	7
3. Clamped square plate with central concentrated load.....	9
4. Cantilever plate with concentrated edge load.....	13
5. Determination of the curvature and twists from known slopes.....	14
6. Determination of deflections.....	15
7. Moiré effect.....	16
8. Schematic diagrams for Moiré principle.....	17
9. Values of $\frac{\phi L}{\Delta}$ at various points on model.....	18
10. Effect of location of camera lens on $\frac{\phi L}{\Delta}$ .....	20
11. Rotation of plate to give photograph which is light throughout.....	21
12. Rotation of plate to give photograph showing original grid.....	21
13. Moiré fringes for cantilever plate.....	22
14. General view of apparatus.....	25
15. General view of apparatus.....	25
16. Uniformly spaced straight Moiré fringes.....	26
17. Supports for simply supported square plate and clamped square plate.....	28
18. Arrangement for simple support.....	29
19. Support for cantilever plate.....	29
20. Loading devices.....	30
21. Actual view of loading arrangement.....	31
22. Square calibration plate.....	32
23. Equally spaced fringe pattern.....	32
24. Actual view of square calibration plate.....	34
25. Support for circular clamped plate.....	34
26. Relation between deflection and load.....	36
27. Fringe pattern for simply supported square plate.....	38
28. Plot of $\frac{\partial w}{\partial x}$ fringe values against $x$ .....	39
29. Plot of $\frac{\partial w}{\partial y}$ fringe values against $y$ .....	40
30. Plot of $\frac{\partial^2 w}{\partial x^2}$ value against $x$ .....	41
31. Distribution of $M_x/P$ , $M_y/P$ for simply supported square plate.....	44
32. Distribution of $M_{xy}/P$ for simply supported square plate.....	45



Figure	Page
33. Fringe pattern for clamped square plate.....	46
34. Distribution of $M_x/P$ , $M_y/P$ for clamped square plate.....	47
35. Distribution of $M_{xy}/P$ for clamped square plate.....	48
36. Deflection profiles for cantilever plate.....	49
37. Distribution of $M_x/P$ , $M_y/P$ in cantilever plate.....	50



LIST OF TABLES

Table	Page
1. Values of $\phi$ and error resulting from using $\phi = \frac{\Delta}{2L}$ for cylindrically curved screen.....	19
2. Moments in a simply supported square plate.....	51
3. Moments in a clamped square plate.....	52
4. Moments and deflections for a cantilever plate.....	53



## NOTATIONS

a Side dimension of square plate.

b Distance from plate model to camera lens.

c Distance from horizontal axis of Moiré set-up to a given point on the model.

d Spacing of lines on the grid.

D  $= Et^3/12(1-\mu^2)$ , Flexural rigidity of a plate.

$D_C$  Flexural rigidity for the calibration plate.

E Modulus of elasticity

L Horizontal distance measured along the camera axis, from plate model to the Moiré screen.

$M_x, M_y$  Bending moments per unit length of sections of a plate perpendicular to x and y axes, respectively.

$M_{xy}$  Twisting moment per unit length of section of a plate perpendicular to x axis.

P Concentrated load.

$Q_x, Q_y$  Shearing forces parallel to z axis per unit length of sections of a plate perpendicular to x and y axes, respectively.

r Radius of calibration plate.

R Concentrated corner force.

t Thickness of the plate

w Deflection of the plate

x, y, z Rectangular coordinates.

$\mu$  Poisson's ratio.

$\lambda$  Spacing of grid used in the difference procedure.

$\phi$  Slope of plate model, or change in slope at a point, in radians.



## I. INTRODUCTION

The general theory of bending of a laterally loaded thin plate has been developed for a number of special cases. In many practical design problems, owing to the difficulty of formulation of the boundary conditions and the solutions of the partial differential equation for plates, analytical solutions are difficult to obtain. Various numerical methods or experimental investigations of models seem to involve too much work for solving practical problems in a reasonably short time. In recent years, an experimental method, the so called Moiré method, has been developed. This method, described by Ligtenberg (1),\* provides sufficient data for the determination of moments in a plate of arbitrary form and loading. The same method was also applied to square clamped plates with or without square cutouts for the determination of moments and deflections by Bradley (2) (3), to flat slabs for the determination of moments by Vreedenburgh (15), and to cantilever plates to determine stresses by Palmer (4). The application of Moiré method to the determination of displacement was described by Weller and Shepard (11). The same method was applied to the strain analysis by Morse, Durelli, and Sciammarella (12), and similar work was also introduced by Low and Bray (13). The application of the Moiré method to determine transient stress

---

\* Numbers in parentheses refer to the bibliography at the end of this thesis.



and strain problem was recently discussed by Riley and Durelli (14). In this study, the Moiré method was used to determine the bending moments and twisting moments in a simply supported square plate and a clamped square plate subjected to central concentrated loads. Bending moments and deflections in a cantilever plate subjected to a concentrated load at the middle of the free edge opposite to the clamped edge was also studied by this method.

Results from this experimental work were compared with Navier solution (6) for the simply supported square plate, Timoshenko's solution (6) for the clamped plate, and Holl's finite difference solution (10) for the cantilever plate respectively.

According to Bradley's work (3) on the bending of plastic plates with uniform or concentrated loading for various boundary conditions, the agreement of deflection and moments as found by the finite difference method and Moiré method was good, the maximum variation was about ten per cent. Ligtenberg found out in most cases (except very near the built-in edges of the model), the accuracy was about 5 per cent of the maximum moment. Observing these results, it is believed that the Moiré method is quite a useful tool for solving plate problems.

The aims of this study can be summarized as follows:

- a. To study the applicability of the Moiré method to metal plates, particularly those with simple or clamped supports, in order to determine its accuracy.



- b. To determine the distribution of moments and compare the results with those obtained by theoretical methods.
- c. To develop the technique of this method by using metal models.

Although the basic principles of the Moiré method were given in Ligtenberg's article as well as Bradley's, they are reviewed here for the completeness of the presentation.

The equipment used and the methods followed in this investigation will be described in some detail in the following chapters.



## II. THEORETICAL ANALYSIS

### 1. Plate Theory.

The ordinary theory of bending of thin elastic, homogeneous isotropic plates requires that the deflected neutral surface of the plate shall satisfy the plate equation (6),

$$\frac{\partial^4 w}{\partial x^4} + 2 \frac{\partial^4 w}{\partial x^2 \partial y^2} + \frac{\partial^4 w}{\partial y^4} = \frac{q}{D} \quad 1$$

in which  $w$  is the deflection of the plate,  $q$  is the intensity of load, and  $D$  is the flexural rigidity of plate.

The derivation of equation 1 is based upon the following assumptions:

- a. The plate material is elastic, homogeneous, and isotropic.
- b. The material obeys Hooke's Law.
- c. The normal stresses in the direction perpendicular to the plane of the plate can be disregarded.
- d. Lines perpendicular to neutral surface before bending remains so after bending.
- e. Plate must be in equilibrium at all times.
- f. The deflections of a plate are small in comparison with its thickness.
- g. There are no membrane forces in the middle plane of the plate. This plane remains neutral during bending.

Now consider an element of the plate which is bent under transverse loading. Taking the positive directions as shown in Fig. 1, in which, the middle plane is taken to coincide with



xy plane, it can be shown that (6):

$$M_x = -D \left( \frac{\partial^2 w}{\partial x^2} + \mu \frac{\partial^2 w}{\partial y^2} \right) \quad 2$$

$$M_y = -D \left( \frac{\partial^2 w}{\partial y^2} + \mu \frac{\partial^2 w}{\partial x^2} \right) \quad 3$$

$$M_{xy} = M_{yx} = -D (1-\mu) \frac{\partial^2 w}{\partial x \partial y} \quad 4$$

$$Q_x = -D \frac{\partial}{\partial x} \left( \frac{\partial^2 w}{\partial x^2} + \frac{\partial^2 w}{\partial y^2} \right) \quad 5$$

$$Q_y = -D \frac{\partial}{\partial y} \left( \frac{\partial^2 w}{\partial x^2} + \frac{\partial^2 w}{\partial y^2} \right) \quad 6$$

$$v_x = -D \left[ \frac{\partial^3 w}{\partial x^3} + (2-\mu) \frac{\partial^3 w}{\partial x \partial y^2} \right] \quad 7$$

$$v_y = -D \left[ \frac{\partial^3 w}{\partial y^3} + (2-\mu) \frac{\partial^3 w}{\partial y \partial x^2} \right] \quad 8$$

$$R = 2D (1-\mu) \frac{\partial^2 w}{\partial x \partial y} \quad 9$$

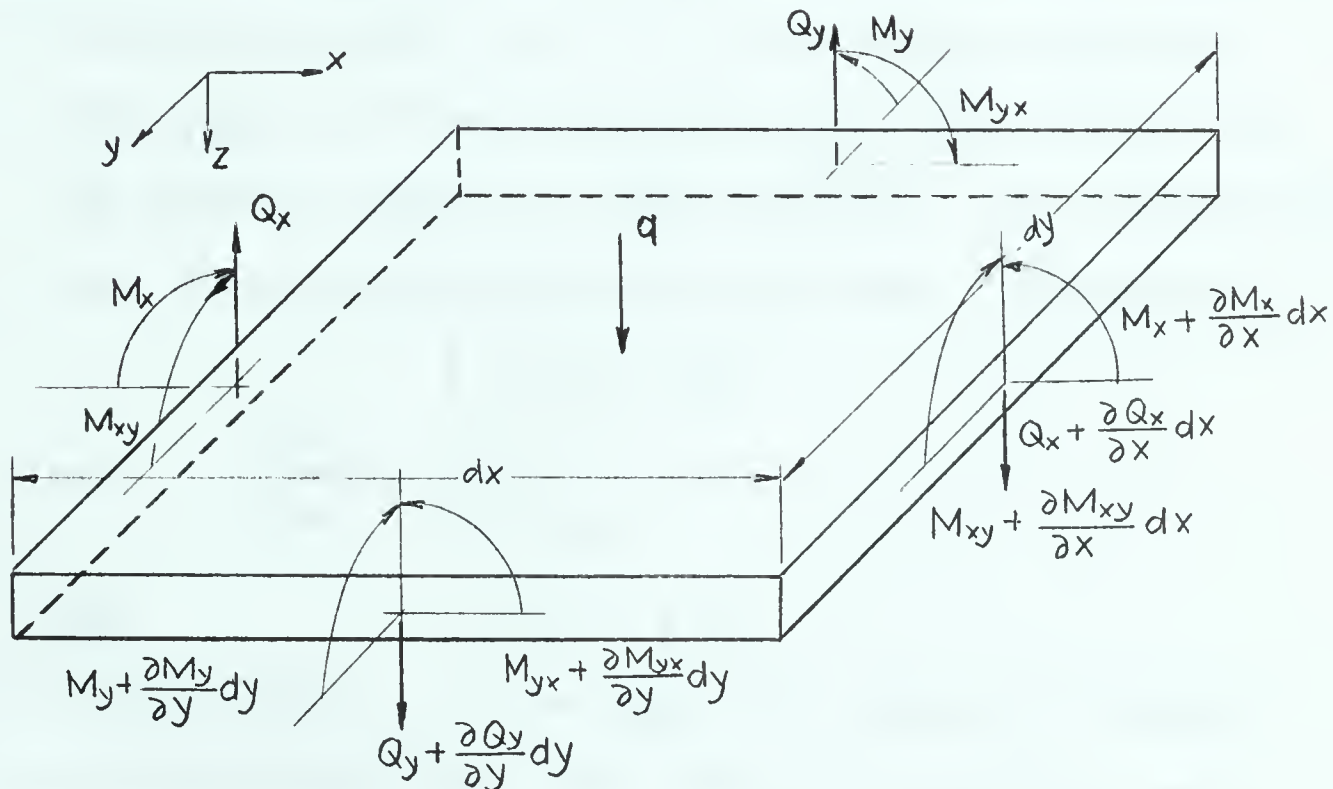


Fig. 1. The element of a plate.

In these expressions  $M_x$ ,  $M_y$  are the bending moments per unit length of sections of a plate perpendicular to  $x$  and  $y$  axes respectively,  $M_{xy}$  and  $M_{yx}$  being the twisting moments;



$Q_x$ ,  $Q_y$  are the shear forces;  $v_x$  and  $v_y$  are the Kirchhoff shears, and  $R$  is defined as the concentrated corner force. Thus, a complete analysis of a plate bent by a lateral load  $q$  is reduced to the integration of Eq. 1. The degree of difficulty in performing this integration depends mostly on the boundary conditions existing along the edges of the plate.

## 2. Boundary Conditions.

The edge of a plate may be free, simply supported, elastically supported, clamped, etc. In this study, the simply supported and clamped edges were investigated. In the case of the cantilever plate, a condition of free edge was involved. The study of these three boundary conditions will now be considered.

a. Simply supported edge. If the edge of the plate along the  $y$  axis, at  $x = 0$ , is simply supported, this edge is free to rotate about the  $y$  axis, and the bending moment  $M_x$  will be zero. All the deflections on this edge will also be zero. Therefore at  $x = 0$ :

$$\left[ M_x \right]_{x=0} = 0$$

or 
$$\left[ \frac{\partial^2 w}{\partial x^2} + \mu \frac{\partial^2 w}{\partial y^2} \right]_{x=0} = 0$$

and 
$$\left[ w \right]_{x=0} = 0$$

b. Clamped edge. If the edge of a plate is clamped, the deflection and slope along the edge are zero. Let the  $y$  axis be clamped, then the boundary conditions are:

$$\left[ w \right]_{x=0} = 0 \quad \left[ \frac{\partial w}{\partial x} \right]_{x=0} = 0$$

c. Free edge. If an edge of a plate, say, the edge  $x = 0$  is entirely free. The boundary conditions existing at



a free edge are:

$$[M_x]_{x=0} = 0 \quad \text{or} \quad \left[ \frac{\partial^3 w}{\partial x^2} + \mu \frac{\partial^2 w}{\partial y^2} \right]_{x=0} = 0$$

$$\text{and} \quad \left[ \frac{\partial^3 w}{\partial x^3} + (2 - \mu) \frac{\partial^3 w}{\partial x \partial y^2} \right]_{x=0} = 0$$

In order that a check of the experimental results may be given, Navier solution for the simply supported square plate, Young's solution for the clamped square plate, and Holl's solution for the cantilever plate by the finite difference method were considered.

### 3. Solutions.

Simply supported square plate. The deflection of a simply supported square plate with central concentrated load was given by Navier in the form of a double trigonometric series (6),

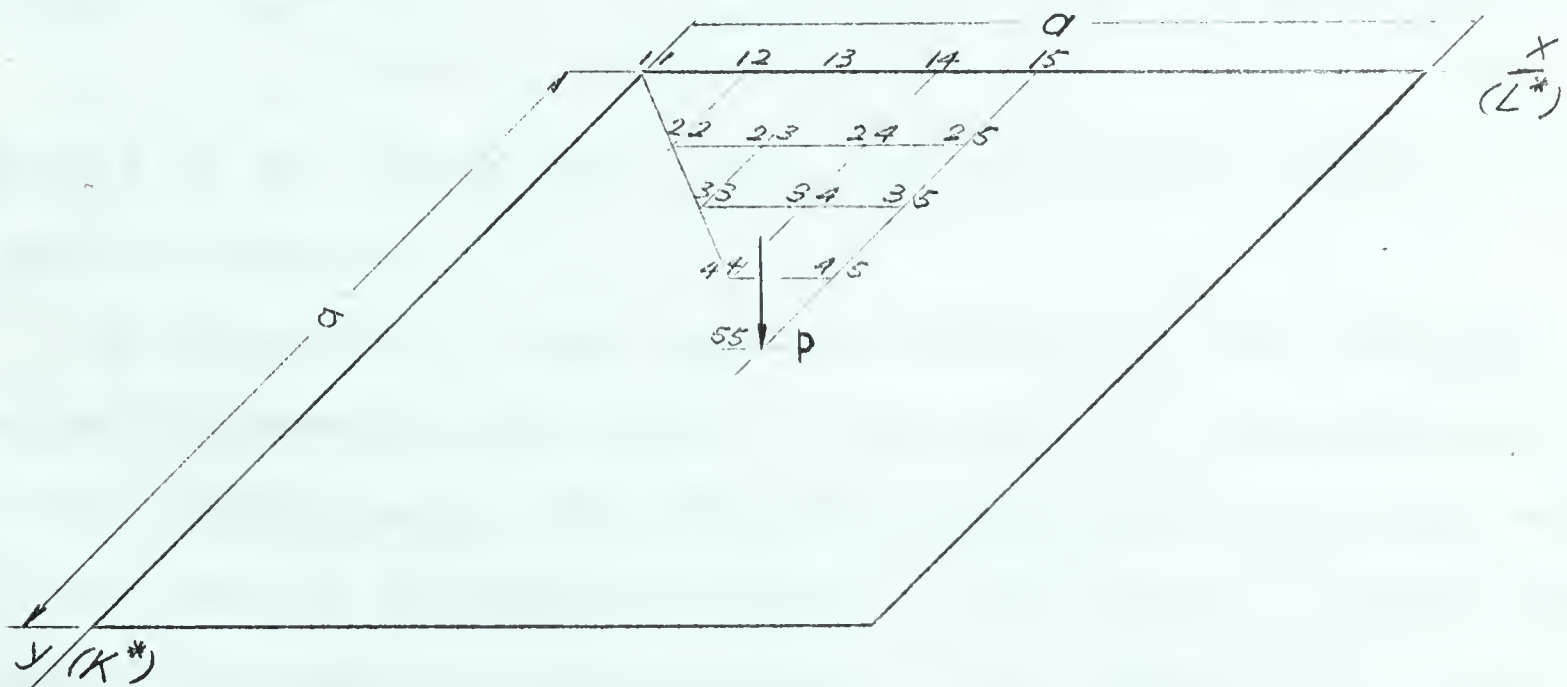


Fig. 2. Simply supported square plate with load P at the center. Showing co-ordinate axes and net points.

$$w = \frac{4Pa^2}{\pi D} \sum_{m=1,3,5}^{\infty} \sum_{n=1,3,5}^{\infty} \frac{\sin \frac{m\pi}{2} \sin \frac{n\pi}{2}}{(m^2 + n^2)^2} \sin \frac{m\pi x}{a} \sin \frac{n\pi y}{a}$$

10

\*Co-ordinates to be used in computation.



which satisfies the plate equation and boundary conditions.

The series converges rapidly, and the deflection at any point of the plate can be obtained with sufficient accuracy by taking only the first few terms of the series. For example, if the first four terms of the series were taken, the maximum deflection is about 3 1/2 percent less than the correct value.

The expressions for bending and twisting moments can be obtained from the general solution 10 by using Equations 2, 3, and 4. These are as follows:

$$M_x = \frac{4P}{\pi^2} \sum_{m=1,3,5}^{\infty} \sum_{n=1,3,5}^{\infty} \frac{(m^2 + \mu n^2)}{(m^2 + n^2)^2} \sin \frac{m\pi}{2} \sin \frac{n\pi}{2} \sin \frac{m\pi x}{a} \sin \frac{n\pi y}{a}$$

$$M_y = \frac{4P}{\pi^2} \sum_{m=1,3,5}^{\infty} \sum_{n=1,3,5}^{\infty} \frac{(n^2 + \mu m^2)}{(m^2 + n^2)^2} \sin \frac{m\pi}{2} \sin \frac{n\pi}{2} \sin \frac{m\pi x}{a} \sin \frac{n\pi y}{a}$$

$$M_{xy} = - \frac{4(1-\mu)}{\pi^2} \sum_{m=1,3,5}^{\infty} \sum_{n=1,3,5}^{\infty} \frac{mn}{(m^2 + n^2)^2} \sin \frac{m\pi}{2} \sin \frac{n\pi}{2} \cos \frac{m\pi x}{a} \cos \frac{n\pi y}{a}$$

where  $P$  is the concentrated load,  $\mu$  is the Poisson's ratio,  $a$  is the length of the plate.

As Timoshenko (6) and Nadai (8) pointed out, the infinite series representing the moments in the case of a concentrated load do not converge well. The numerical computation for  $M_x$ ,  $M_y$ , and  $M_{xy}$  was done by an IBM-1620 computer. The computer programs and results of computation are presented in the Appendix 1. In the computation, values of  $m$ , and  $n$  were taken up to 29. From the result of the calculations, it was found that the series did not converge well along the centre lines,  $x = \frac{a}{2}$ ,  $y = \frac{a}{2}$ . In fact, the series for  $M_x$ , and  $M_y$  at the centre, 55, were divergent.



For the numerical computation, it is evident from symmetry that the computation needs only be extended over an area of one-eighth of the plate. Values of  $M_x$ ,  $M_y$ , and  $M_{xy}$  are tabulated in Table 2.

Clamped square plate. A general method of solution for rectangular plates with clamped edges and an arbitrary loading has been developed by Timoshenko (6). Results of calculation using his method for maximum deflection, moments, and edge shears have been given by Young (7).

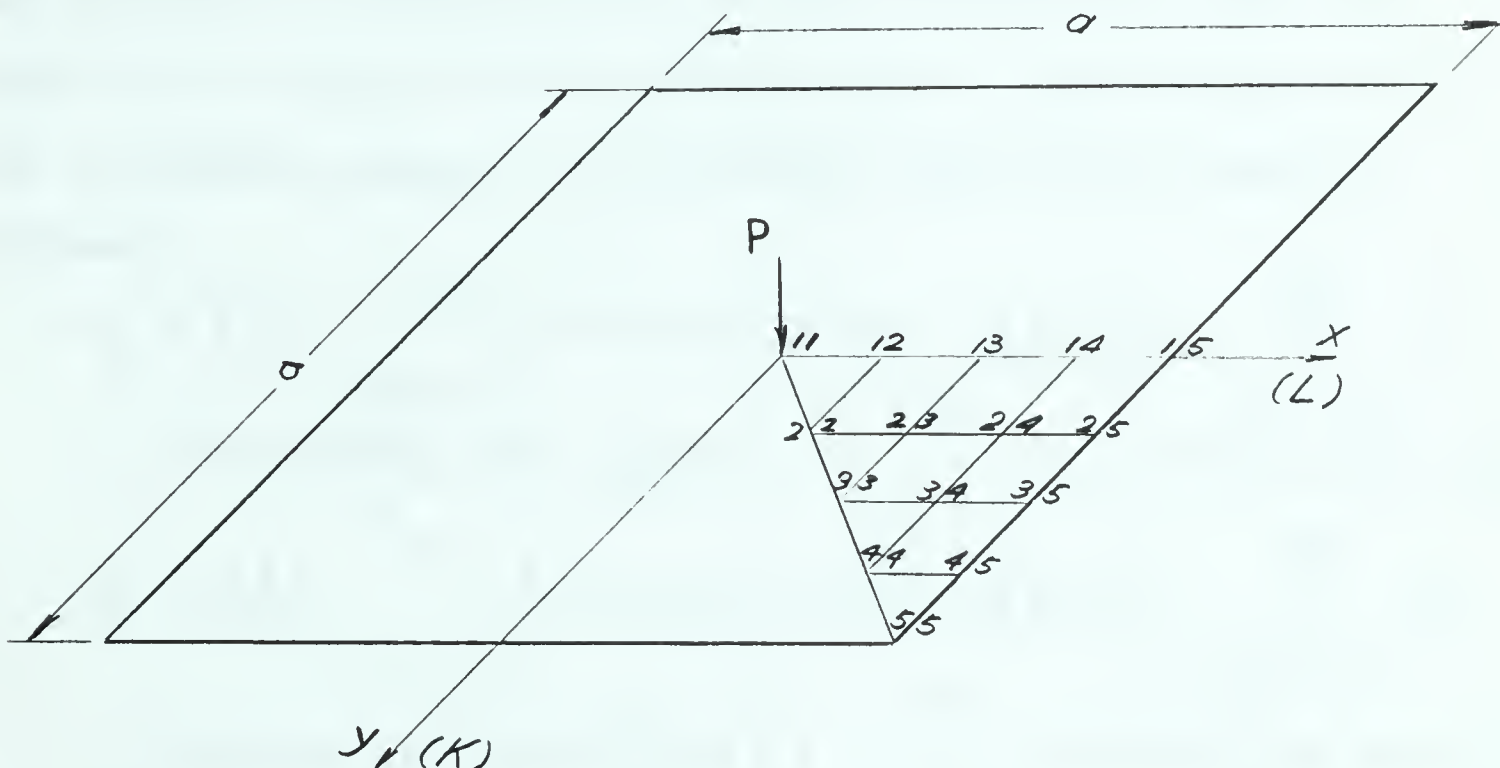


Fig. 3. Clamped square plate with central concentrated load. Showing coordinate axes and net points.

The solution of this particular case is expressed as follows:

$$\begin{aligned}
 w &= w_1 + w_2 + w_3 \quad (7) \\
 &= \frac{Pa^2}{2\pi^3 D} \sum_{m=1,3,5}^{\infty} \frac{1}{m^3} \cos \frac{m\pi x}{a} \left[ \left( \tanh \alpha_m - \frac{\alpha_m}{\cosh^2 \alpha_m} \right) \cosh \frac{m\pi y}{a} \right. \\
 &\quad \left. - \sinh \frac{m\pi y}{a} - \tanh \alpha_m \frac{m\pi y}{a} \sinh \frac{m\pi y}{a} + \frac{m\pi y}{a} \cosh \frac{m\pi y}{a} \right] \\
 &\quad - \frac{a^2}{2\pi^2 D} \sum_{m=1,3,5}^{\infty} A_m \frac{(-1)^{(m-1)/2}}{m^2 \cosh \alpha_m} \cos \frac{m\pi x}{a} \left[ \frac{m\pi y}{a} \sinh \frac{m\pi y}{a} \right.
 \end{aligned}$$



$$-\alpha_m \tanh \alpha_m \cosh \frac{m\pi y}{a} \Big] - \frac{a^2}{2\pi^2 D} \sum_{m=1,3,5}^{\infty} B_m \frac{(-1)^{(m-1)/2}}{m^2 \cosh \alpha_m} \cos \frac{m\pi y}{a} \left[ \frac{m\pi x}{a} \sinh \frac{m\pi x}{a} - \alpha_m \tanh \alpha_m \cosh \frac{m\pi x}{a} \right] \quad 11$$

in which  $w_1$  is identified with the elastic surface of a rectangular plate carrying a concentrated load  $P$  in the centre of a plate and satisfying Navier's boundary conditions  $w_1=0$  and  $\frac{\partial^2 w_1}{\partial x^2} + \mu \frac{\partial^2 w_1}{\partial y^2} = 0$  along the edges. This first portion of the solution contains a singularity at the center of the plate, where the bending moments become infinite, while the terms  $w_2$  and  $w_3$  have no singularities in the interior or along the edges of the plate (8). By using solution 11 and Eqs. 2, 3, and 4, bending moments, and twisting moments are found as follows:

$$M_x = \frac{P}{2} \left[ \frac{1}{\pi} \sum_{m=1,3,5}^{\infty} \frac{1}{m} \cos(\beta x) \left\{ \varphi(\beta y) - \mu \psi_1(\beta y) \right\} - \sum_{m=1,3,5}^{\infty} A \cos(\beta x) \left\{ \psi_2(\beta y) - \mu \psi_3(\beta y) \right\} + \sum_{m=1,3,5}^{\infty} B \cos(\beta y) \left\{ \theta_1(\beta x) - \mu \theta_2(\beta x) \right\} \right]$$

$$M_y = \frac{P}{2} \left[ \frac{1}{\pi} \sum_{m=1,3,5}^{\infty} \frac{1}{m} \cos(\beta x) \left\{ \mu \varphi(\beta y) - \psi_1(\beta y) \right\} - \sum_{m=1,3,5}^{\infty} A \cos(\beta x) \left\{ \mu \psi_2(\beta y) - \psi_3(\beta y) \right\} + \sum_{m=1,3,5}^{\infty} B \cos(\beta y) \left\{ \mu \theta_1(\beta x) - \theta_2(\beta x) \right\} \right]$$

$$M_{xy} = \frac{(1-\mu)P}{2} \left[ \frac{1}{\pi} \sum_{m=1,3,5}^{\infty} \sin(\beta x) \eta_1(\beta y) - \sum_{m=1,3,5}^{\infty} A \sin(\beta x) \eta_1(\beta y) - \sum_{m=1,3,5}^{\infty} B \sin(\beta y) \zeta(\beta x) \right]$$

where

$$\alpha_m = \frac{m\pi}{2}$$

$$\beta = \frac{m\pi}{a}$$

$$\mu = \text{Poisson's ratio}$$



$$\varphi(\beta y) = (\tanh \alpha_m - \frac{\alpha_m}{\cosh^2 \alpha_m}) \cosh(\beta y) - \sinh(\beta y) - \tanh \alpha_m \frac{m\pi y}{a} \sinh(\beta y) + \frac{m\pi y}{a} \cosh(\beta y)$$

$$\psi_1(\beta y) = (\tanh \alpha_m - \frac{\alpha_m}{\cosh^2 \alpha_m}) \cosh(\beta y) - 2 \tanh \alpha_m \cosh(\beta y) - \tanh \alpha_m \frac{m\pi y}{a} \sinh(\beta y) + \sinh(\beta y) + \frac{m\pi y}{a} \cosh(\beta y)$$

$$\psi_2(\beta y) = \frac{m\pi y}{a} \sinh(\beta y) - \alpha_m \tanh \alpha_m \cosh(\beta y)$$

$$\psi_3(\beta y) = 2 \cosh(\beta y) + \frac{m\pi y}{a} \sinh(\beta y) - \alpha_m \tanh \alpha_m \cosh(\beta y)$$

$$\theta_1(\beta x) = 2 \cosh(\beta x) + \frac{m\pi x}{a} \sinh(\beta x) - \alpha_m \tanh \alpha_m \cosh(\beta x)$$

$$\theta_2(\beta x) = \frac{m\pi x}{a} \sinh(\beta x) - \alpha_m \tanh \alpha_m \cosh(\beta x)$$

$$\eta_1(\beta y) = (\tanh \alpha_m - \frac{\alpha_m}{\cosh^2 \alpha_m}) \sinh(\beta y) - \tanh \alpha_m \sinh(\beta y) - \tanh \alpha_m \frac{m\pi y}{a} \cosh(\beta y) + \frac{m\pi y}{a} \sinh(\beta y)$$

$$\eta_2(\beta y) = \sinh(\beta y) + \frac{m\pi y}{a} \cosh(\beta y) - \alpha_m \tanh \alpha_m \sinh(\beta y)$$

$$\rho(\beta x) = \sinh(\beta x) + \frac{m\pi x}{a} \cosh(\beta x) - \alpha_m \tanh \alpha_m \sinh(\beta x)$$

$$A = \frac{PA_m(-1)^{\frac{m-1}{2}}}{\cosh \alpha_m} = B$$

$$A_1 = B_1 = -0.1025 \quad A_3 = B_3 = 0.02630 \quad A_5 = B_5 = 0.00420$$

$$A_7 = B_7 = 0.0015 \quad A_9 = B_9 = 0.00055 \quad A_{11} = B_{11} = 0.00021$$

$$A_{13} = B_{13} = 0.00006$$

Again the series representing the bending moments did not converge well along the centre lines  $x = 0$ , and  $y = 0$ , except at points  $(0, \frac{a}{2})$ ,  $(\frac{a}{2}, 0)$ ,  $(0, -\frac{a}{2})$ , and  $(-\frac{a}{2}, 0)$ . The series for bending moments were divergent at the centre point 11. Values for  $M_x$ ,  $M_y$ , and  $M_{xy}$  are given in Table 2. Computer program and results of computation are provided in Appendix 2.

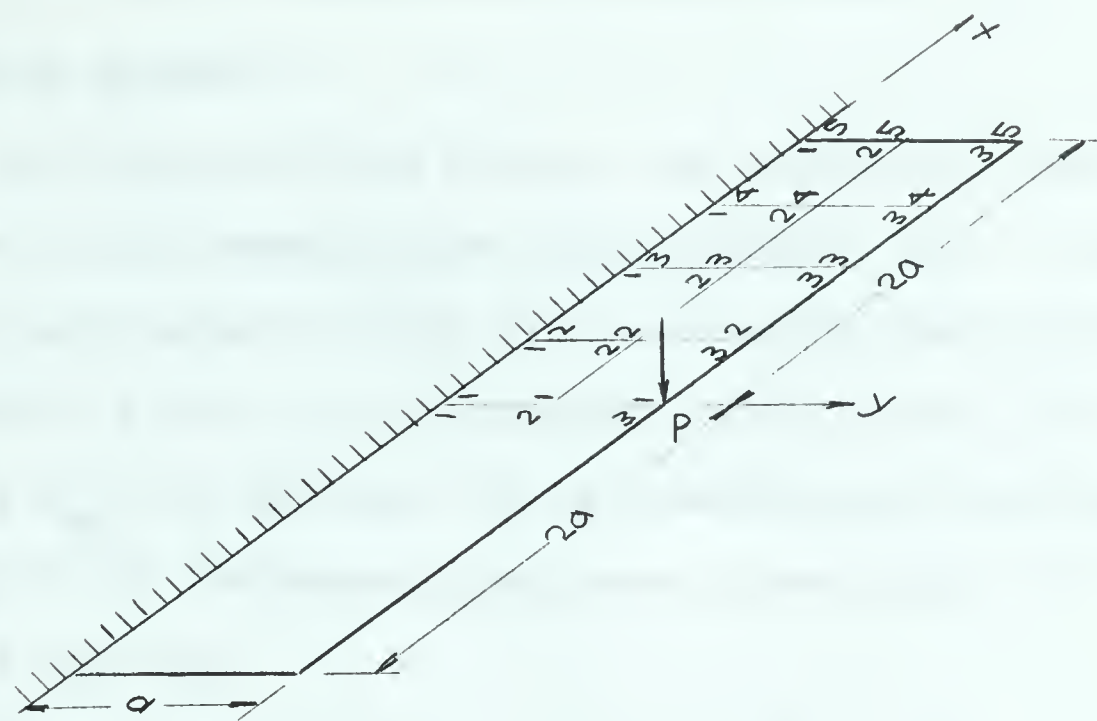
According to the calculation, the result seems to disagree



with Timoshenko's argument that the moments with four correct figures may be obtained by using seven coefficients A and seven coefficients B (6).

Cantilever plate. Because of the free corners, it seems that the problem of the bending of a cantilever plate of finite dimensions is difficult to solve from the standpoint of a bi-harmonic analysis. However, various approximate methods have been applied to this kind of problem. The finite difference analysis of a cantilever plate with a span-to-chord ratio of 1:4 and loaded by a concentrated force at the middle of the longitudinal free edge was presented by Holl (10). This problem requires a solution of  $\nabla^4 w = 0$ , and all boundary conditions to be satisfied. An approximate solution was attempted by dividing the plate into square nets of width  $\lambda = \frac{a}{2}$ , as indicated in the right half of the plate in Fig. 4. The results of the calculations are given in Table 4. and represented graphically in Fig. 36, and Fig. 37.



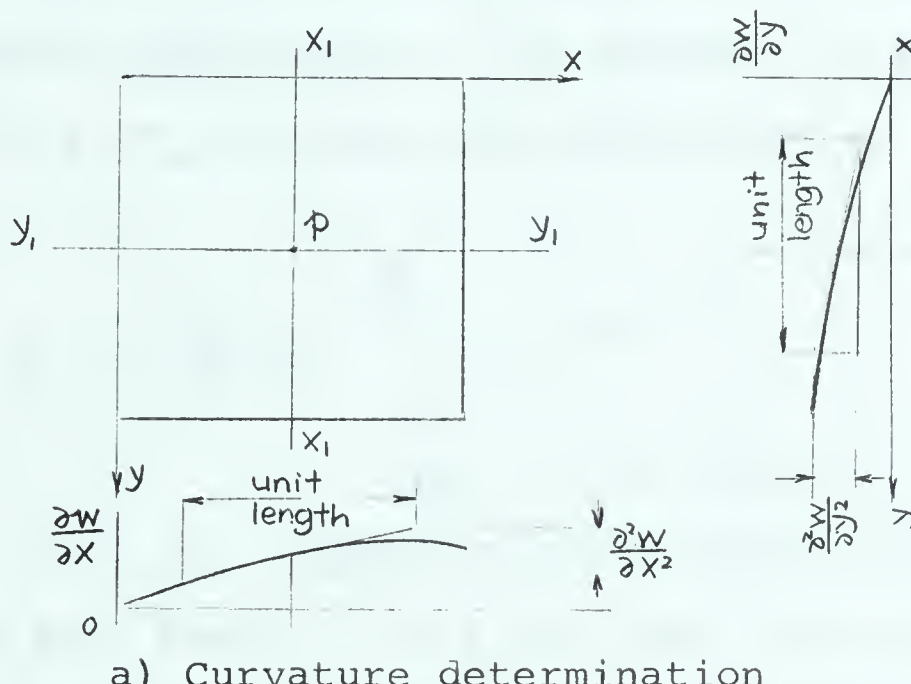




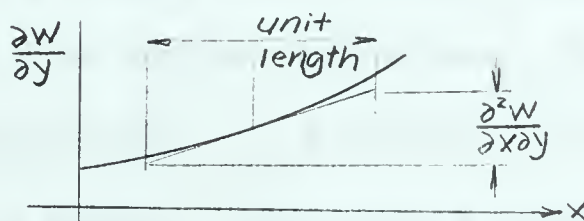
## III. EXPERIMENTAL INVESTIGATION

## 1. The Moiré method.

From the theory of thin plates, the equations relating the deflections to the moments are given by Eqs. 2, 3 and 4. The moments are determined by differentiating the slopes. If, at some point,  $p (x_1, y_1)$ , in a plate (Fig. 5) (8), the moments  $M_x$ ,  $M_y$ , and  $M_{xy}$  are desired, it is possible to find them if the curvatures of the deflected plate were known along the direction  $x_1, -x_1$ , and  $y_1, -y_1$ .



a) Curvature determination



b) Twist determination

Fig. 5. Determination of the curvature and twists from known slopes.

The curvature in the  $x$  direction is approximately  $\frac{\partial^2 w}{\partial x^2}$ ,

which can be found from the slope of the  $\frac{\partial w}{\partial x}$  versus  $x$  curve.



Similarly  $\frac{\partial^2 w}{\partial y^2}$  can be found from the slope of the  $\frac{\partial w}{\partial y}$  versus  $y$  curve. These curvatures, along with the constant,  $D$  and  $\mu$ , can be used to find  $M_x$  and  $M_y$ .

In order to determine the twisting moment  $M_{xy}$ , it is necessary to know the twist,  $\frac{\partial^2 w}{\partial x \partial y}$ ; this can be approximated at point  $p$ , as shown in Fig. 5., by plotting the values of  $\frac{\partial w}{\partial y}$  along the line  $y_1 - y_1$  and finding the slope at point  $p$ , or similarly by plotting  $\frac{\partial w}{\partial x}$  along  $x_1 - x_1$ .

Knowing the slopes along a line in the plate, it is possible to determine the deflections. For example, in Fig. 6, if the deflection at  $a$ ,  $w_a$  is known, the deflection at  $a'$  will be:

$$w_{a'} = w_a + \int_a^{a'} \frac{\partial w}{\partial x} dx$$

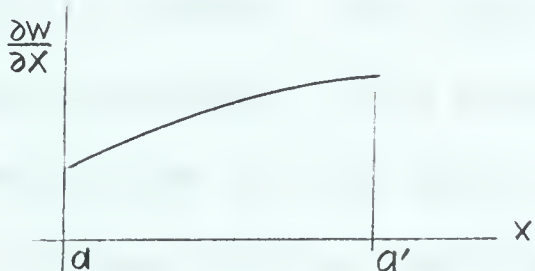


Fig. 6. Determination of deflections.

in which the last term of the right hand side is the area under the  $\frac{\partial w}{\partial x}$  versus  $x$  curve and can be found by a planimeter.

Thus once the slopes have been found for all points in the plate, it is possible to find deflections, moments and shears throughout the plate. The Moiré method provides the means for finding these slopes.

The Moiré or "watered silk" effect is an optical phenomenon produced by the "mechanical interference" of two somewhat similar arrays of dots or lines. The result of this effect is the pattern of alternate dark and white fringes as shown in Fig. 7.



This fringe pattern gives the changes in slopes of the surface due to the application of a load, and from this, the curvatures and the deflections can be determined as previously mentioned.

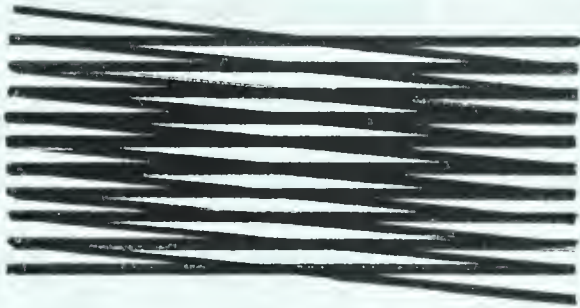


Fig. 7. Moiré effect.

In this method, the essential elements are a ruled screen, a camera, and a mirrored model plate.

In testing, the model was used as a mirror to observe a ruled screen. If the model is loaded, the image on the ground glass of the camera will be distorted. The change of the image was caused by the deflection of the plate model. The difference between the two images can be recorded by superimposing the photographs for the unloaded and the loaded state on the same negative. If a suitable ruling was chosen for the screen, "Moiré" fringes will appear. With a special form of the screen, these can be interpreted as contour lines for the first derivative of  $w$  ( $l$ ).

The moments are linear functions of the second derivatives of  $w$ . These are first derivatives of slope  $\phi$  and can easily be determined (as illustrated in Fig. 5). For determining the moments, the plate bending rigidity  $D$  must also be known.

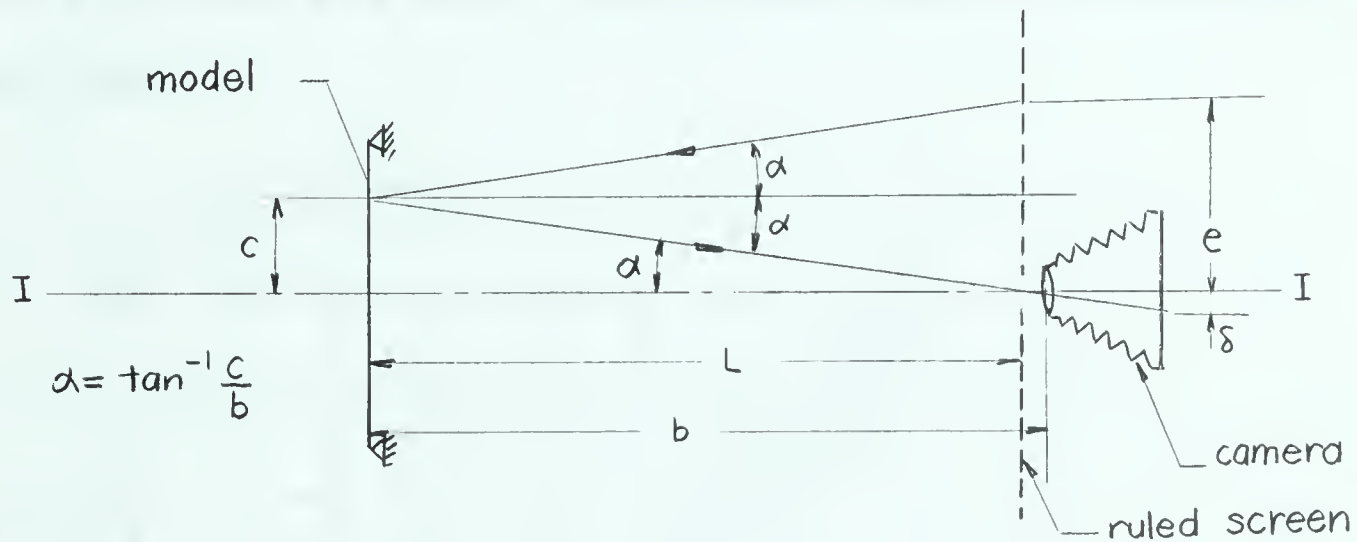
In order to find the change in slope  $\phi$  of the model



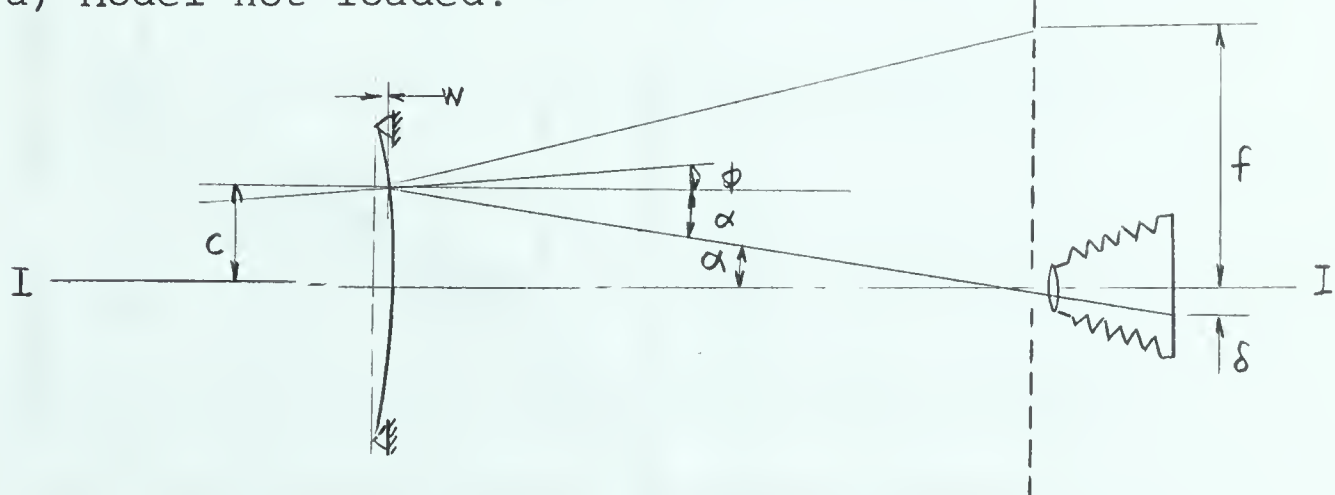
from the unloaded condition (Fig. 8a) to the loaded condition (Fig. 8b), the difference between  $f$  and  $e$  must be obtained, where  $e$  is the distance from the axis I-I of the point on the surface of the ruled screen reflected to the photographic negative by a point  $p$  on the unloaded model, and  $f$  is the distance to the point on the screen reflected by the same point  $p$  with the model loaded. For a flat screen,

$$\Delta = f - e = 2L\phi \left[ 1 + \frac{c^2}{b^2} \right] \quad (1), \quad (2) \quad 12$$

where  $\phi$  is the change in slope of the deflected plate. Expression 12 will still be valid when the initial slope of the model is not zero (2).



a) Model not loaded.



b) Model loaded.

Fig. 8. Schematic diagrams for Moire principle.



If the point  $p$  on the plate is not too great a distance from the axis, the term  $\frac{c^2}{b^2}$  will be very small and can be neglected for a flat screen. For example, with  $b=25$  in. and with an 8 inch model (i.e., maximum  $c=4$  in), an error of about 2.5 per cent would result if  $\phi$  were taken equal to  $\frac{\Delta}{2L}$ . However, this error can be reduced to a negligible amount by the use of a curved screen, as suggested by Ligtenberg (1).

For a cylindrical screen of radius equal to  $3.5 L$ , the values of  $\phi$  will be approximately equal to  $\frac{\Delta}{2L}$ . As shown in Fig. 9, and Fig. 10 (2), if the model is of such a size that its extreme point is  $0.2 L$  from the axis, the maximum error will be about 0.05 per cent.

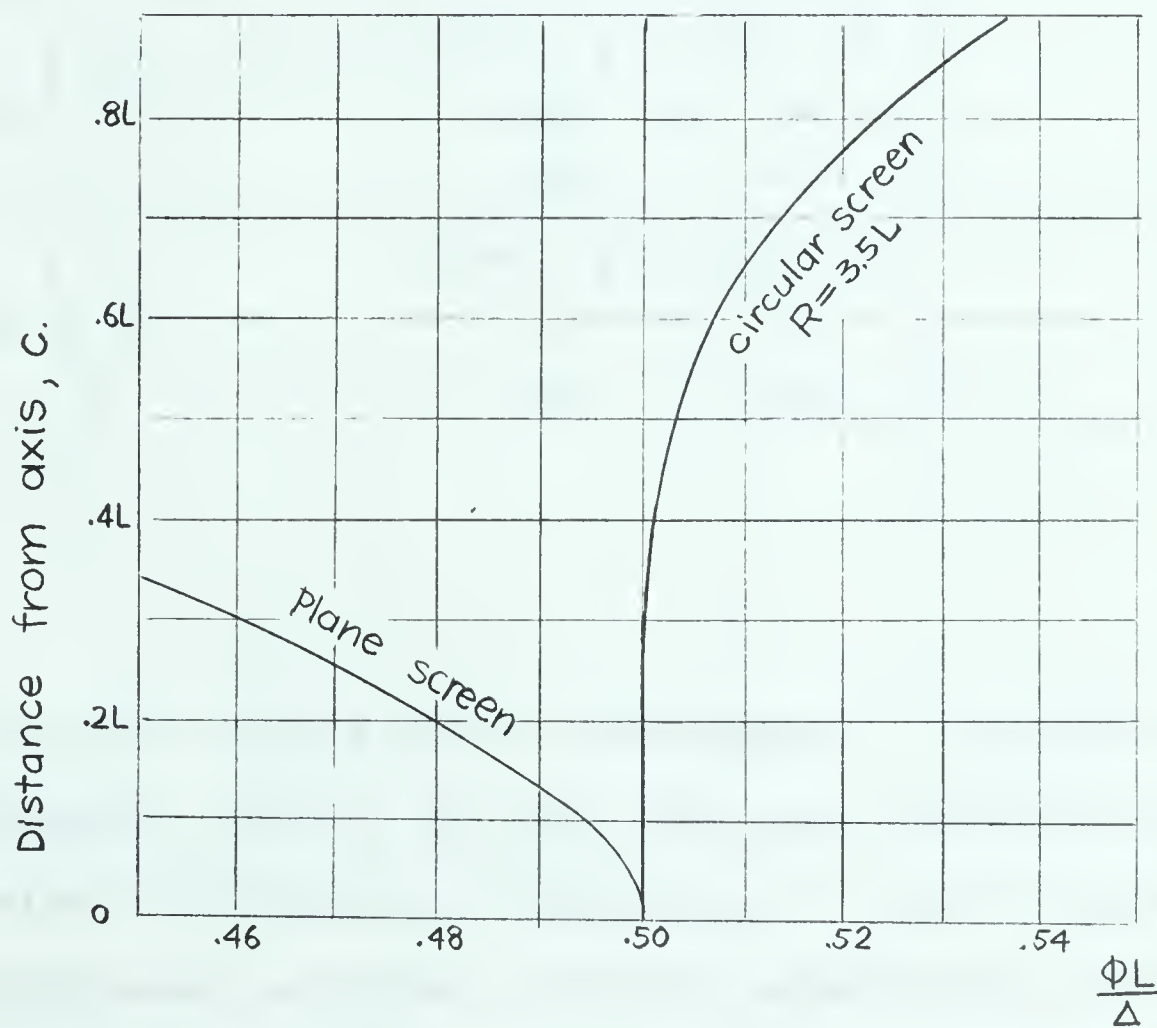


Fig. 9. Values of  $\frac{\phi L}{\Delta}$  at various points on model (for  $b=L$ )



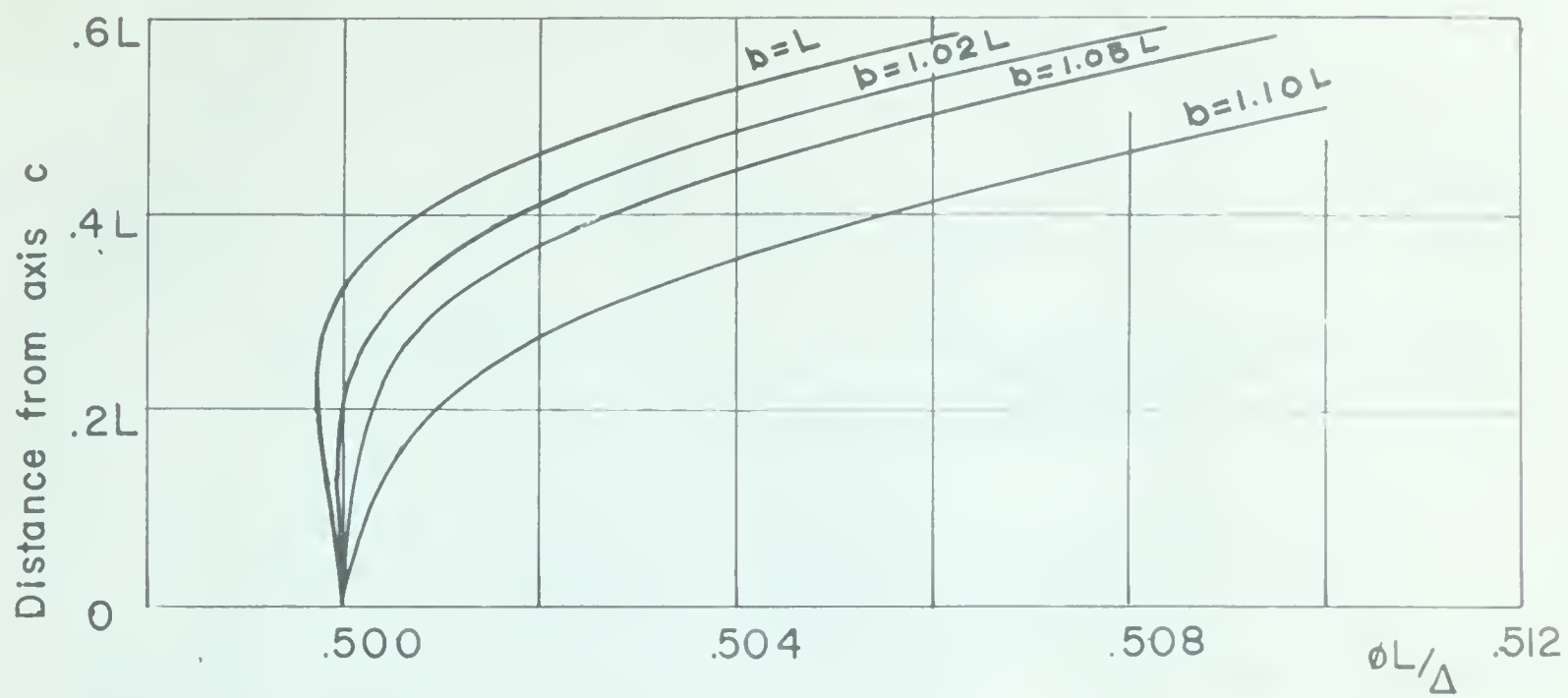
$b$  (Fig. 8) may not actually be equal to  $L$ , but, for practical reasons may be greater. The effect of  $b$  on the value of  $\frac{\phi L}{\Delta}$  was calculated by Bradley (2), and the result is represented graphically in Fig. 10 and tabulated in table 1.

TABLE 1. VALUES OF  $\phi$  AND ERROR (E) RESULTING FROM USING  $\phi = \frac{\Delta}{2L}$  FOR CYLINDRICALLY CURVED SCREEN. RADIUS =  $3.5L$ .

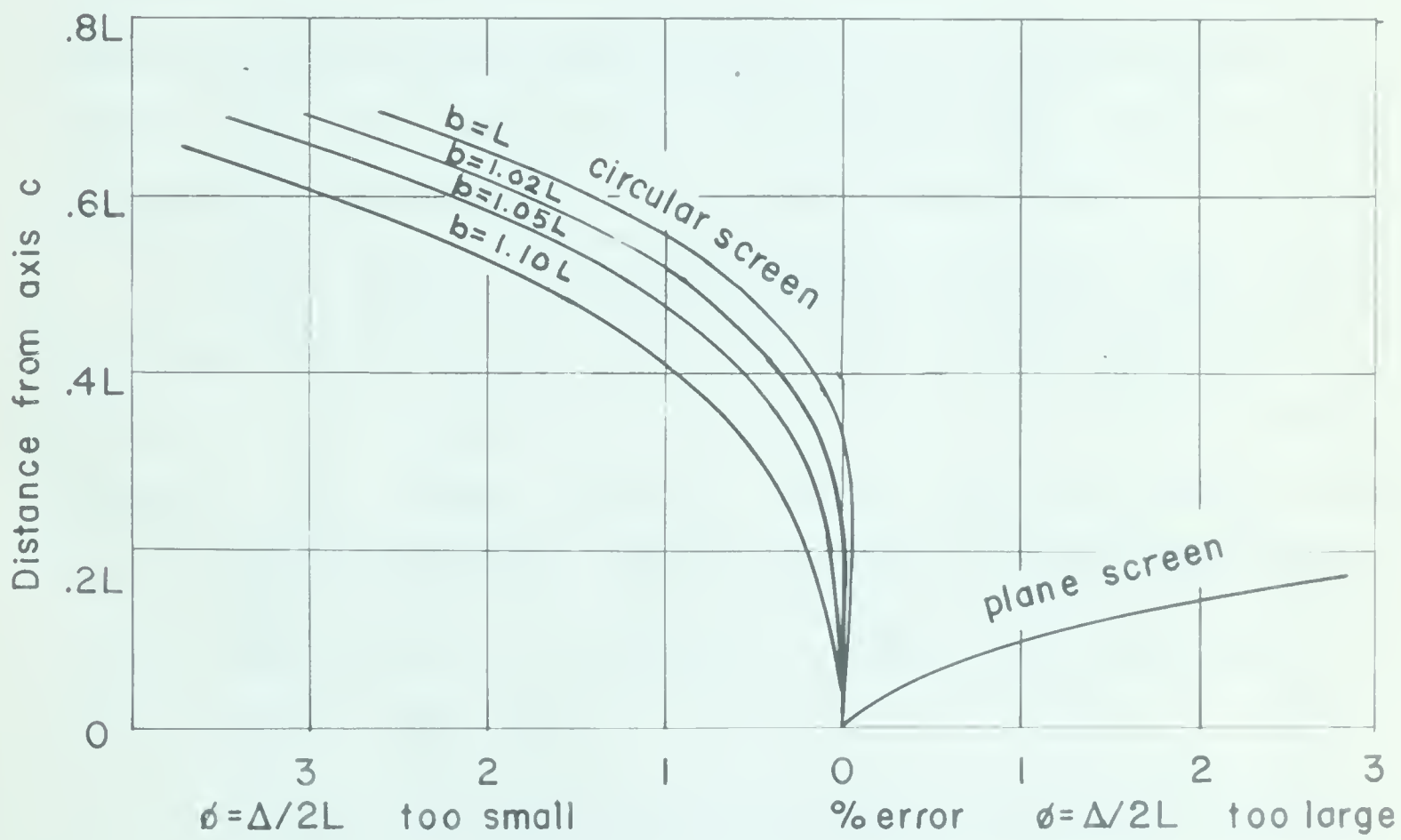
Y		.1L	.3L	.5L	.7L	1.0L
$b=L$	$\phi$	.49993 $\frac{\Delta}{L}$	.49982 $\frac{\Delta}{L}$	.49977 $\frac{\Delta}{L}$	.50035 $\frac{\Delta}{L}$	.50447 $\frac{\Delta}{L}$
	E %	+ .01	+ .04	+ .05	- .07	- .89
	C	.05L	.151L	.254L	.363L	.540L
$b=1.02L$	$\phi$	-	.49998 $\frac{\Delta}{L}$	.50020 $\frac{\Delta}{L}$	-	.50615 $\frac{\Delta}{L}$
	E %	-	+ .004	- .04	-	- 1.22
	C	-	.152L	.257L	-	.544L
$b=1.05L$	$\phi$	-	.50021 $\frac{\Delta}{L}$	.50053 $\frac{\Delta}{L}$	-	.50858 $\frac{\Delta}{L}$
	E %	-	- .042	- .106	-	- .169
	C	-	.155L	.261L	-	.551L
$b=1.10L$	$\phi$	-	.50056 $\frac{\Delta}{L}$	.50180 $\frac{\Delta}{L}$	-	.51241 $\frac{\Delta}{a}$
	E %	-	- 0.112	- .359	-	- 2.420
	C	-	.158L	.266a	-	.562a

In order that  $\phi$  may be determined,  $\Delta$  has to be measured. As an example, in Fig. 11a (2), the first exposure was made with point P reflecting a black line,  $l$ , and if the resulting photograph were developed, it would merely have recorded a reflection of the grid. If the model is rotated after the first





a) Values of  $\phi L / \Delta$  at various points on model circular screen  $R=3.5L$



b) Percentage error resulting from using  $\phi = \Delta / 2L$  for various values of  $b$ .

Fig.10. Effect of location of camera lens on  $\phi L / \Delta$



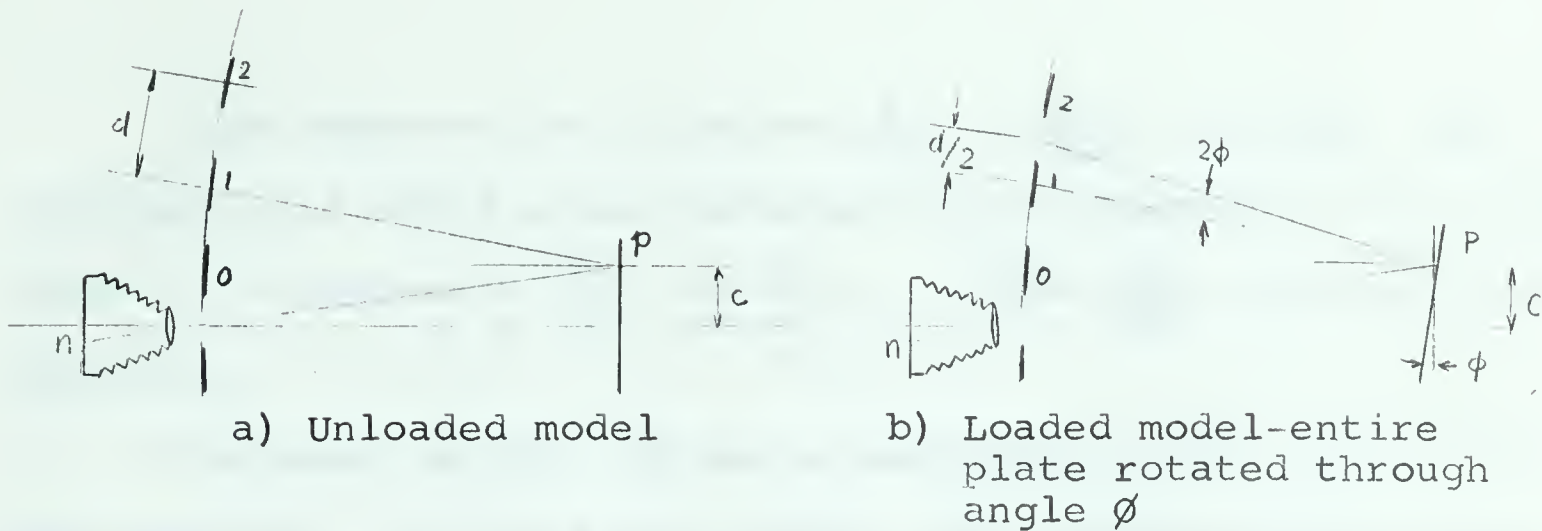


Fig. 11. Rotation of plate to give photograph which is light throughout.

exposure through an angle  $\phi$ , as shown in Fig. 11b, such that a point  $p$  now reflects a white line, and a second exposure is made on the same negative, the result will be a negative which has been sensitized throughout, and a light print will result. In this case,  $\Delta = \frac{1}{2}d$ , and since  $\phi = \frac{\Delta}{2L}$ , then  $\phi = \frac{d}{4L}$ . Therefore, the slope  $\phi$  of the model can be found.

If the model is rotated through a greater angle after the first exposure (Fig. 12) such that a dark line was reflected to the negative by point  $p$ , the film would be sensitized at  $n$  by neither exposure, and a black line would result at  $n$  on the final print; the whole print would simply appear as the grid itself, with alternate light and dark lines. In this case,  $\phi = \frac{\Delta}{2L} = \frac{d}{2L}$ .

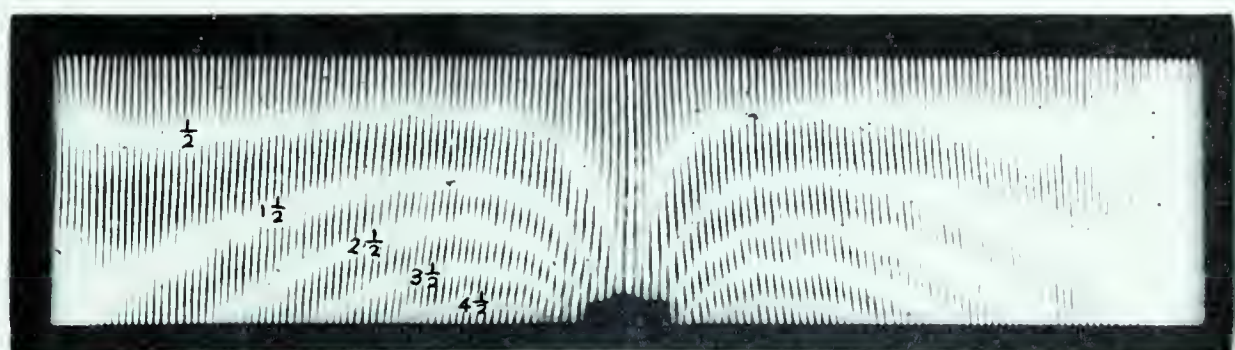


Fig. 12. Rotation of plate to give photograph showing original grid.



Thus whenever the slope was  $\frac{d}{2L}$ ,  $2(\frac{d}{2L})$ , ...  $n(\frac{d}{2L})$ , the original grid would appear with alternate black and white lines. When the slope was  $\frac{1}{2}(\frac{d}{2L})$ ,  $\frac{3}{2}(\frac{d}{2L})$ , ...,  $\frac{2n-1}{2}(\frac{d}{2L})$ , the print will be white.

The model in Fig. 13 was a cantilever plate clamped at the top edge. In the actual model, the slopes varied continuously from point to point, and there resulted on the prints a series of light regions and other regions in which the original grid appeared as shown in Fig. 13.



a) Fringe pattern for slope in x-direction.

b) Fringe pattern for slope in y-direction.

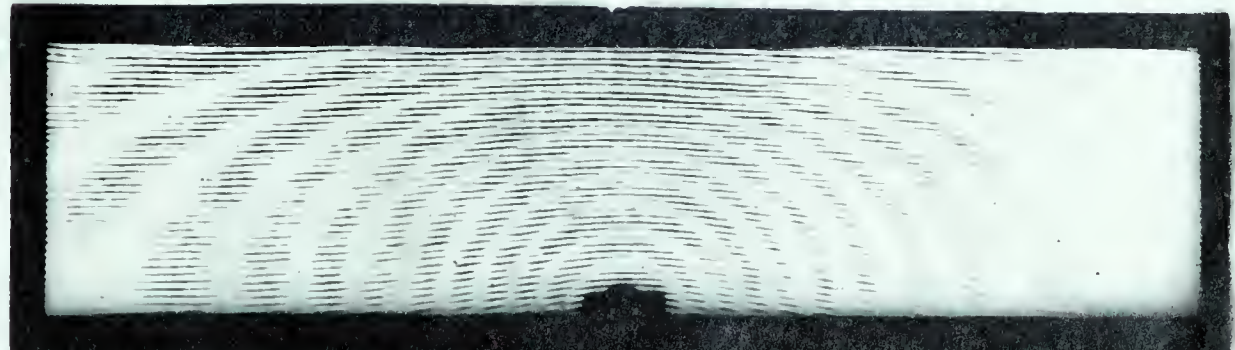


Fig. 13. Moiré fringes for cantilever plate with a concentrated load at the mid-point of the lower edge.  
Load = 10.019 lb. Span-to-chord ratio is 1:4. Aluminum sheet.  
Thickness = 0.0630 in.



In these photographs, regions of the model for which  $\phi = \frac{d}{2L}, 2(\frac{d}{2L}), \dots, n(\frac{d}{2L})$  remained black which received the reflection of a black line in both exposures. For portions which received either the reflection of two white lines, or of one black and one white line, the photograph was white. For points on these lines,  $\phi = \frac{1}{2}(\frac{d}{2L}), \frac{3}{2}(\frac{d}{2L}), \dots$ , etc. In interpreting Fig. 13a, since the top edge is fixed, the fringe for  $\phi = 0$  appears along the clamped edge. Moving downward, the successive dark fringes show all points for which  $\frac{\partial w}{\partial x} = \phi = \frac{d}{2L}, 2(\frac{d}{2L}), \dots$ , etc.; the light fringes show points for which  $\frac{\partial w}{\partial x} = \phi = \frac{1}{2}(\frac{d}{2L}), \frac{3}{2}(\frac{d}{2L}), \dots$ , and so on. For convenience of plotting, the magnitude of these fringes was designated by order numbers as shown.

The relative magnitude of the second derivatives can be obtained by observing the fringe pattern. The fringes for  $\frac{\partial^2 w}{\partial y^2}$  were closer together in the y direction where  $\frac{\partial^2 w}{\partial y^2}$  was greater. Similarly, the fringes for  $\frac{\partial^2 w}{\partial x^2}$  were closer together in the x direction where  $\frac{\partial^2 w}{\partial x^2}$  was greater.

From the two photographs of Fig. 13, it was then possible to find the curvatures,  $\frac{\partial^2 w}{\partial x^2}$  and  $\frac{\partial^2 w}{\partial y^2}$ , and, knowing the load, the dimensions of the model, and the elastic constants of the material, the moments were computed.

## 2. Apparatus.

The design of the test apparatus was adapted from reference (3). For the purpose of testing a metal model, a more rigid structure was required. In this study, the frame was built of  $3 \times 3 \times \frac{1}{4}$  in. steel angles. They were welded and bolted together



as shown in Fig. 14 and Fig. 15. Its overall size was 72 x 36 x 34 in. The distance,  $L$ , from the model to the screen was 25 in. The distance,  $b$ , from model to the lens of the camera was 26.25 in. i.e.,  $b = 1.05 L$ . The ruled screen was 36 x 36 in.

The grid. The grid used was drawn by lining with India ink on a sheet of white paper. For obtaining the clearest Moiré fringes, the width of each line was chosen to be 0.05 in. and the grid spacing,  $d$ , was 0.10 in. Since the ruling interval  $d$  must be the same everywhere, the ordinary method of drafting was believed inadequate to do such accurate work. Ruling was finally achieved with the help of a milling machine and a particular inking device. A Leroy pen, with a specially designed holder, was held steadily to a slider which was allowed to slide smoothly on a steel ruler that was fixed to the frame of the machine. A board was then placed under the ruler and was clamped to the table of the machine. A sheet of poster paper was placed on the board. After a line had been finished, the table was then moved a distance of 0.1 in. ahead by means of a micrometer adjustment, and another line was drawn, and so on.

Finally, the grid was pasted to the curved screen. The radius of this cylindrical surface was 87.5 in. or 3.5  $L$ . The frame of the screen was constructed in such a way that the grid could be quickly rotated through any desired angle; index markings were placed on the back of the frame so that the angular position could be easily determined. For lighting the grid, two No. 2 photoflood bulbs with built-in reflectors were used.



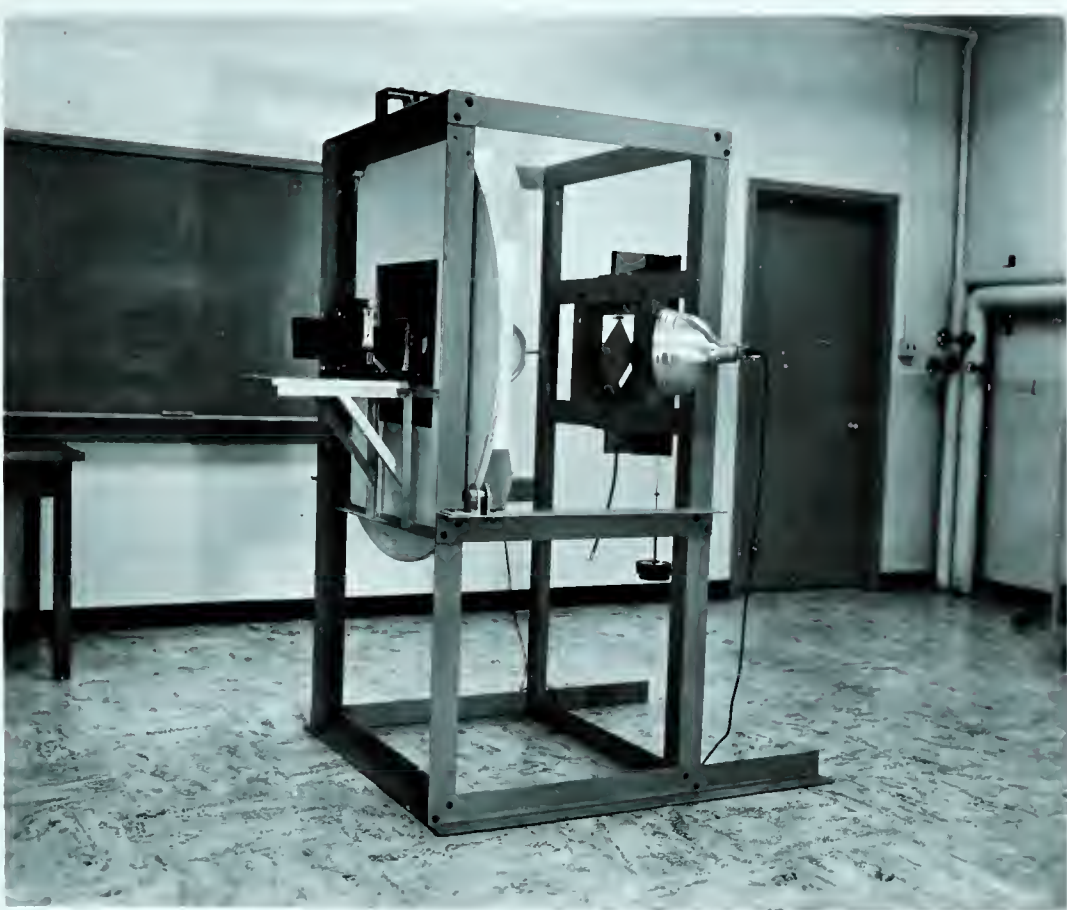


Fig. 14. General view of apparatus.

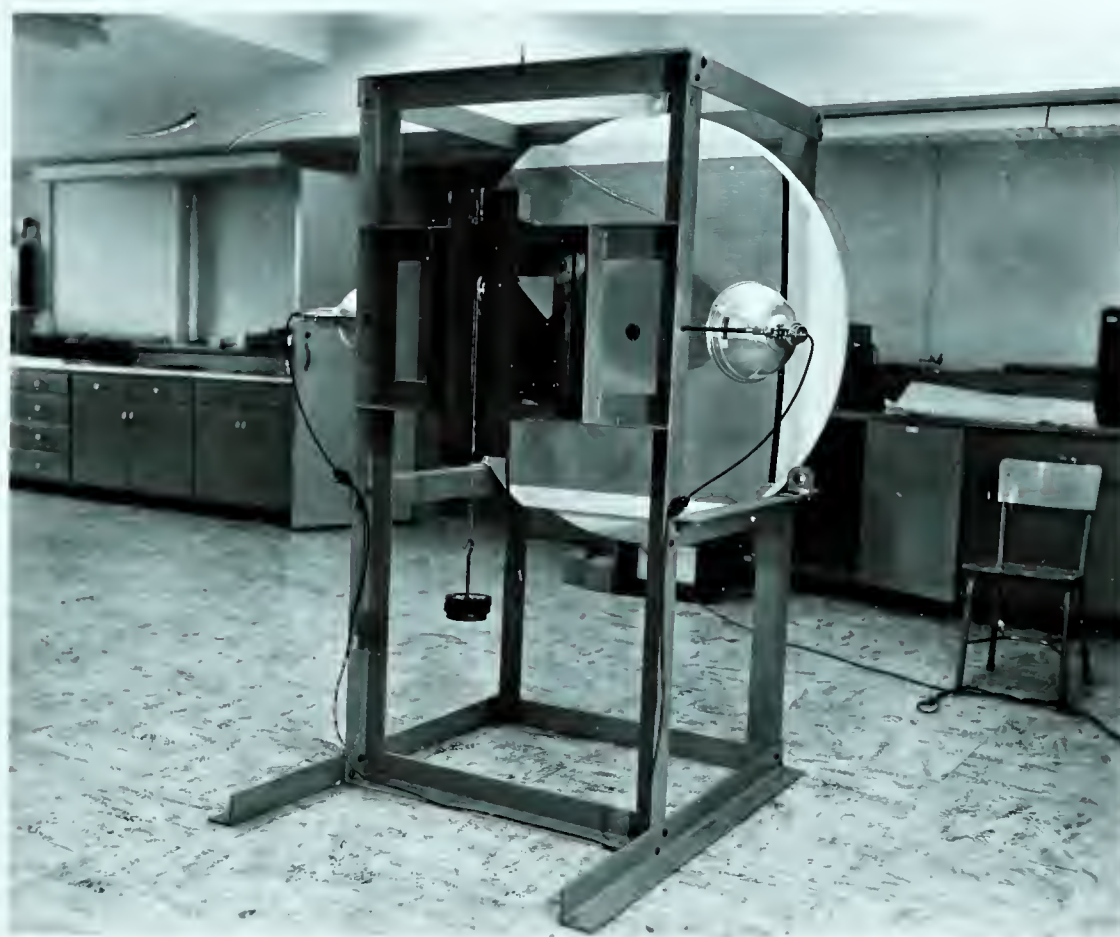


Fig. 15. General view of apparatus. Note the arrangement for application of concentrated load.



A check on the accuracy of the grid was obtained by photographing the screen once, and then after turning it through a small angle (e.g.  $3^\circ$ ) superimposing a second photograph on the first. The result ought to be a pattern of uniformly spaced straight Moiré fringes (1).

Fig. 16 shows that the screen used was quite satisfactory.

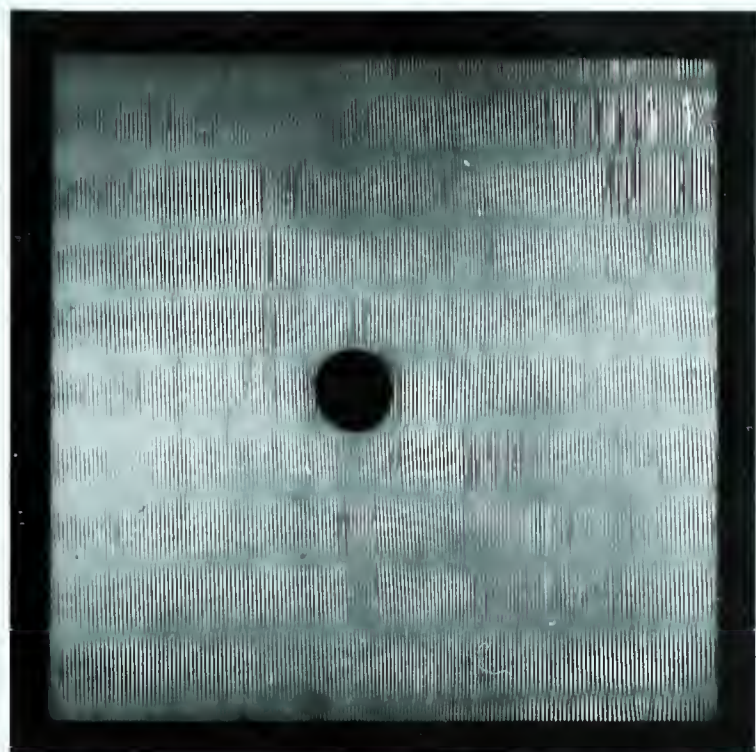


Fig. 16. Uniformly spaced straight Moiré fringes. (angle of rotation= $3^\circ$ )

The camera. The camera used was a 4 x 5 Crown Graphic with a f/5.6, 180 mm lens. The camera was rigidly mounted behind the small hole (diameter=2 in) in the centre of the screen. In order to avoid any possible motion during the exposure or between the two exposures, the shutter was controlled by a metal cable release. When an aperture was 1/45, with Kodak Kodalith Ortho (type 3) sheet films, good negatives were produced with each of the two exposures lasting seven seconds.



Model support. The plate model tested was supported in a vertical position in the test frame. In this thesis, simply supported square plate, clamped square plate, and cantilever plate were investigated. For the clamped square plate, two  $\frac{3}{4}$  in. steel plates were machined as shown in Fig. 17. The centre opening was 9.05 x 9.05 in., and the assembly clamped together with twenty  $\frac{3}{8}$  in. bolts.

For the simply supported edge condition, the fixture was as shown in Fig. 17, and Fig. 18. The model was held vertically at the lower knife edge by two small pins. The bolts were tightened lightly to draw the assembly together. On testing, a small initial load was applied to the model in order to seat it against the front knife edge.

The support for a cantilever plate is shown in Fig. 19. The plate was clamped along the upper edge by four  $\frac{3}{8}$  in. bolts.

Loading mechanism. A concentrated load was applied to the model by means of a lever mechanism, which appears in Fig. 20 and Fig. 21a. Weights were applied to one arm of the lever, and the direction was changed so that a horizontal force  $P$  was applied to the model. The two arms of the lever were not equal, forces were corrected by a factor  $g/h$ .

For the application of concentrated load to the cantilever plates, a slender flexible wire was passed over a pulley, one end of the wire was connected to the plate by a C-clamp as shown in Fig. 20, and Fig. 21b, and load was suspended at the other end.



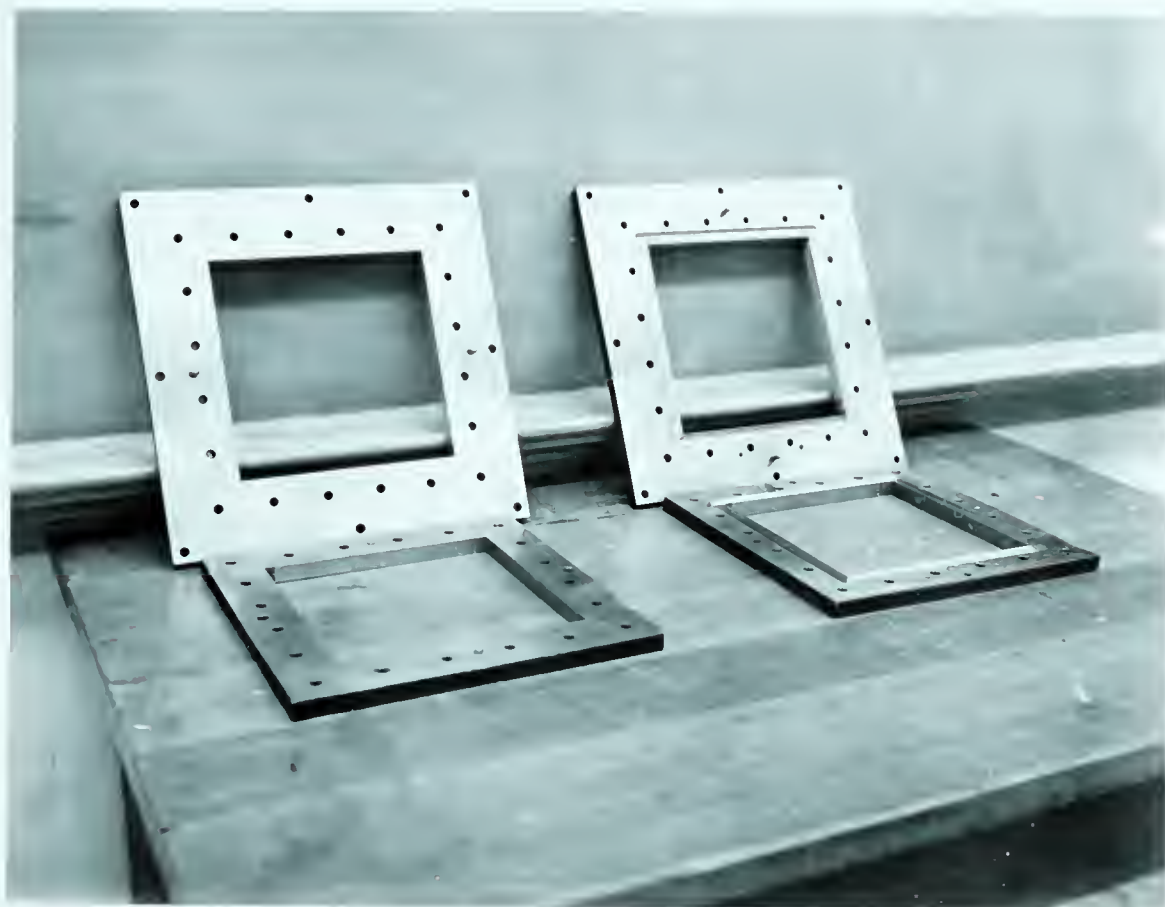


Fig.17. Supports for simply supported square plate (right) and clamped square plate(left).



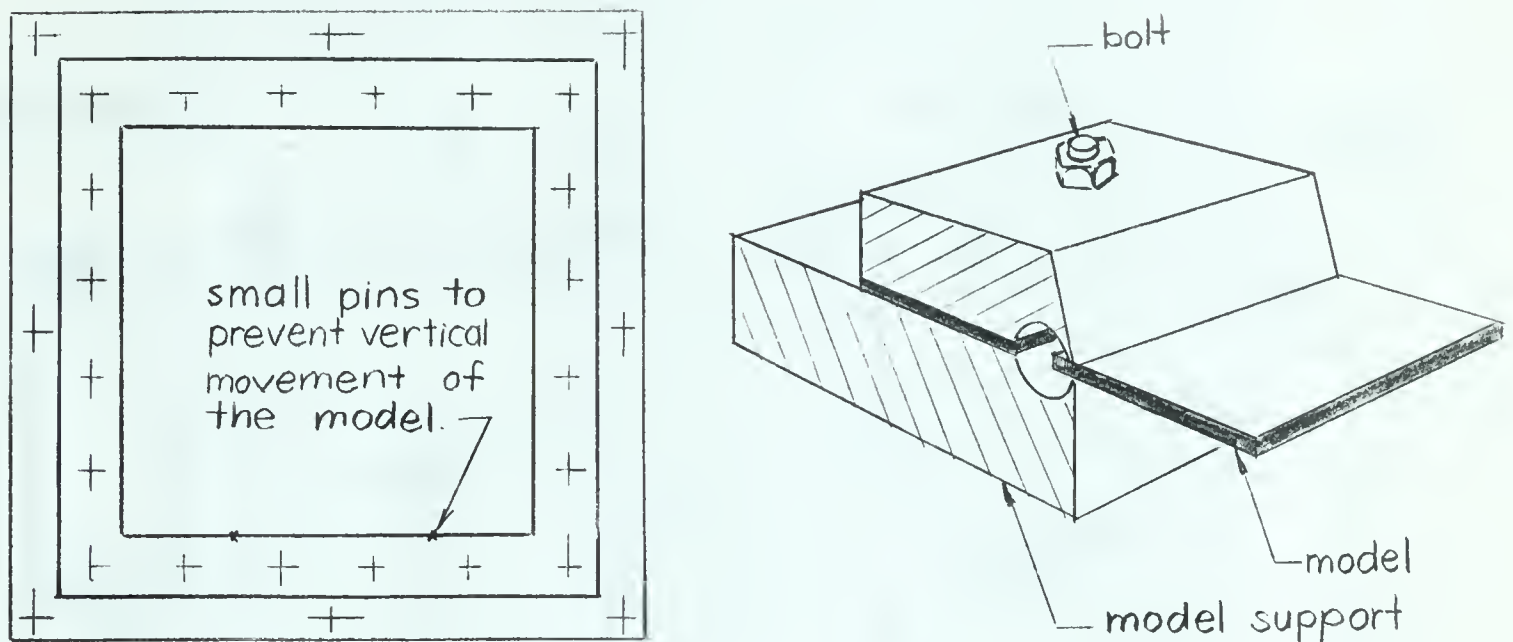


Fig. 18. Arrangement for simple support.

The support for a cantilever plate is shown in Fig. 18. It was secured to the test frame by eight bolts.



Fig. 19. Support for cantilever plate.



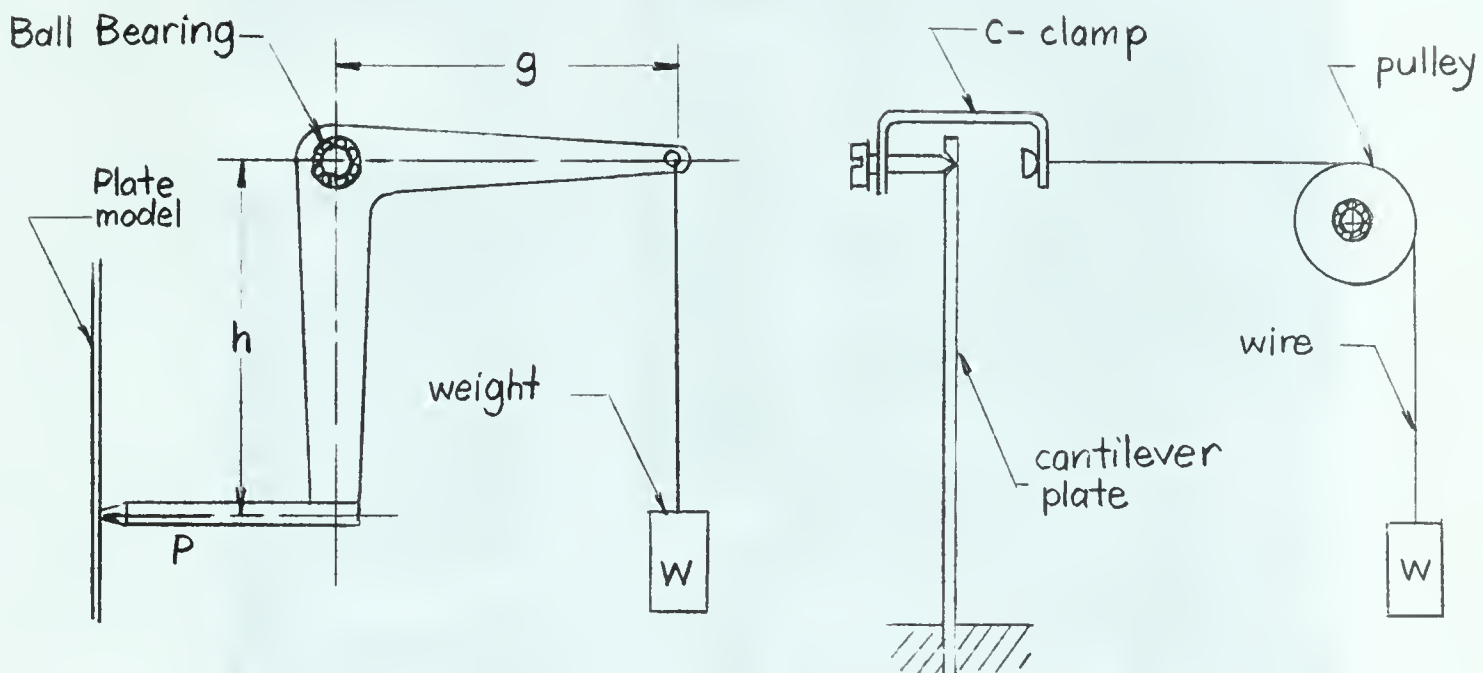
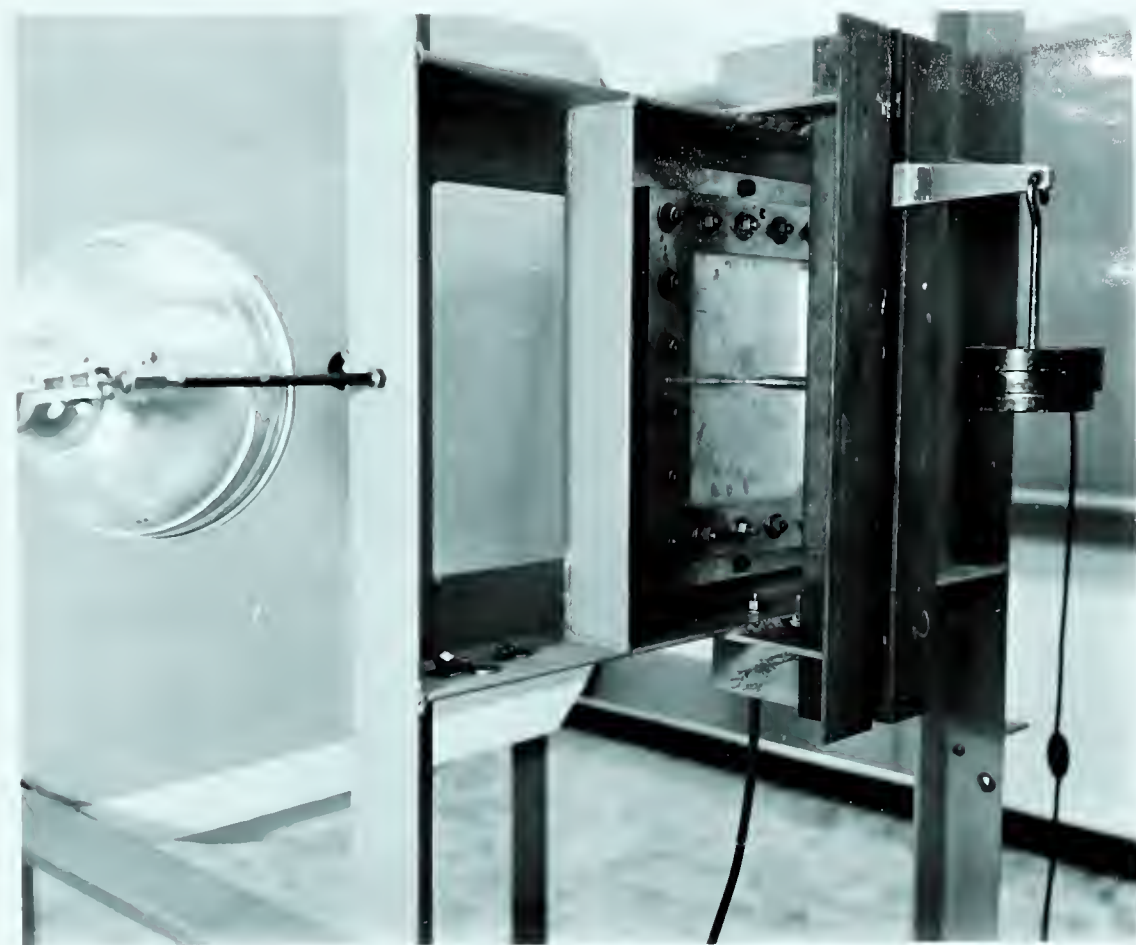


Fig. 20. Loading devices.

The model. The materials used for this investigation were ANACONDA cold rolled 0.0641 in. brass sheet and ALCLAD 7075-T6, QQ-A-287A ALCOA 0.063 in. aluminum sheet. In order to obtain a reflective surface, one side of the model was first polished by a felt wheel which was driven by a  $\frac{1}{4}$  in. hand drill. After that, Silvo silver polish was applied. The plate was polished to such an extent that the image of the grid at a distance of 25 in. away could be seen clearly on the mirroring surface.

The thickness of the sheet to be used is governed somewhat by the fineness of fringe pattern desired with the particular grid being used. Since small deflection theory is no longer applicable with accuracy if the deflections exceed about one-half of the plate thickness (2), a lower limit on the thickness is imposed. On the other hand, the thicker the model, the





a) Lever system.



b) Pulley system.

Fig. 21. Actual view of loading arrangement.



greater will be the loads required to produce suitable fringe pattern for analysis. In this study, the maximum deflection of the plate was confined to be less than  $\frac{1}{32}$  in. which is onehalf the plate thickness.

### 3. Calibration of the material.

It is possible to compute the value of plate rigidity  $D$  from the elastic constants of the model material. However,  $D$  may be determined by using either a square model (Fig. 22, and Fig. 24) or a circular plate (Fig. 25). In Fig. 24 a square plate was supported at three corners, and a concentrated load was applied at the fourth one. The  $x$  and  $y$  axes were taken along the diagonals as indicated, then  $M_x$ ,  $M_y$ , and  $M_{xy}$  are constant everywhere:  $M_x = -M_y = \frac{P}{2}$ ;  $M_{xy} = 0$ .

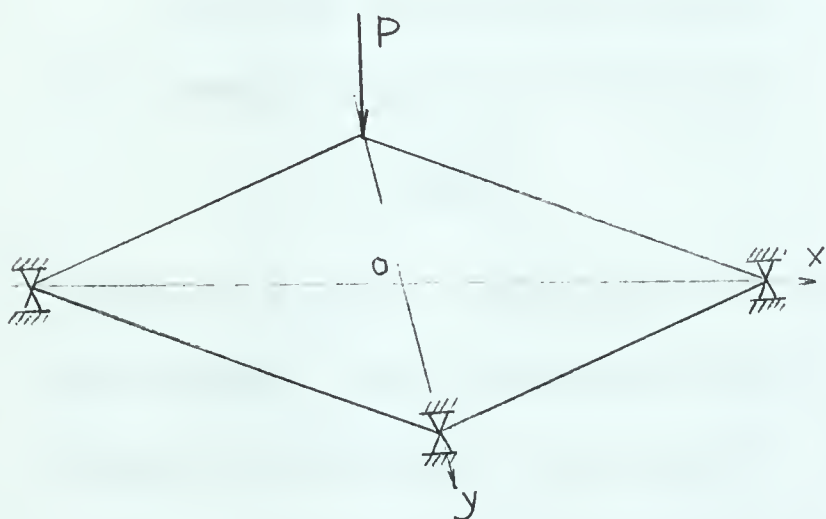


Fig. 22. Square calibration plate.

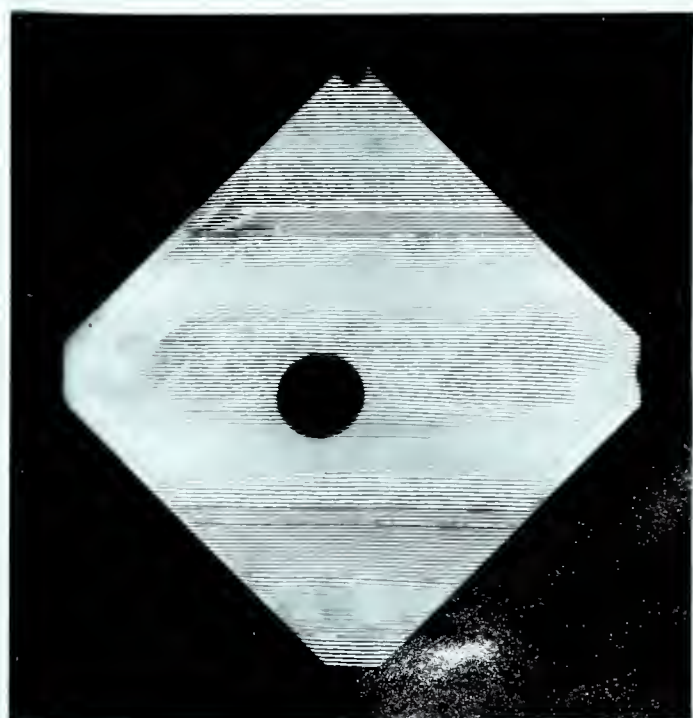


Fig. 23. Equally spaced fringe pattern. Load  $P=0.6$  lb. Brass sheet thickness =0.0641 in.



In this case, the fringes will be straight and equidistant, and spaced a distance  $s_f$  apart (Fig. 23)

Since;  $M_x = -M_y = M$

and from equation 2 , and 3

$$M_x = M = -D \left( \frac{\partial^2 w}{\partial x^2} + \mu \frac{\partial^2 w}{\partial y^2} \right)$$

$$M_y = -M = -D \left( \frac{\partial^2 w}{\partial y^2} + \mu \frac{\partial^2 w}{\partial x^2} \right) ,$$

and solving for D

$$D = - \frac{M}{(1-\mu) \frac{\partial^2 w}{\partial x^2}} , \quad 13$$

where the bending moment

$$M_y = - \frac{P}{2}$$

$$\text{and} \quad \frac{\partial^2 w}{\partial y^2} = \frac{\partial w}{\partial y} = \frac{d}{s_f L}$$

Thus, equation (13) becomes:

$$D_c = D = \frac{P s_f}{2(1-\mu) \left( \frac{d}{s_f L} \right)} . \quad 14$$

For the uniformly loaded circular plate with clamped edges, the centre deflection has been given (6) as,

$$w = \frac{q r^4}{64 D_c}$$

where  $q$  is the intensity of loading, and  $r$  is the radius of the plate. By measuring the centre deflection,  $D$  for the cali-

bration plate was found to be  $D_c = \frac{q r^4}{64 w}$ .

The size of the square plate was 6 x 6 in., the circular plate was 9 in. in diameter. Poisson's ratio for brass was taken to be 0.33. By using square calibration plate, the value of  $D_c$  for brass plate was found to be 468 lb-in. (load  $P=0.6$  lb.),



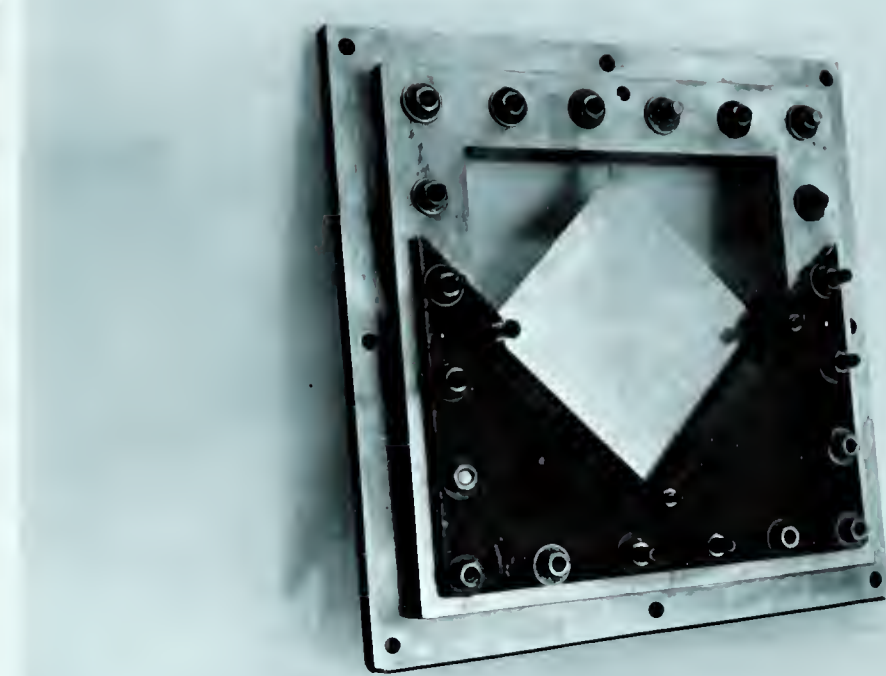


Fig.24. Actual view of square calibration plate. The plate is supported at three corner points and a concentrated load applied at the fourth corner point.

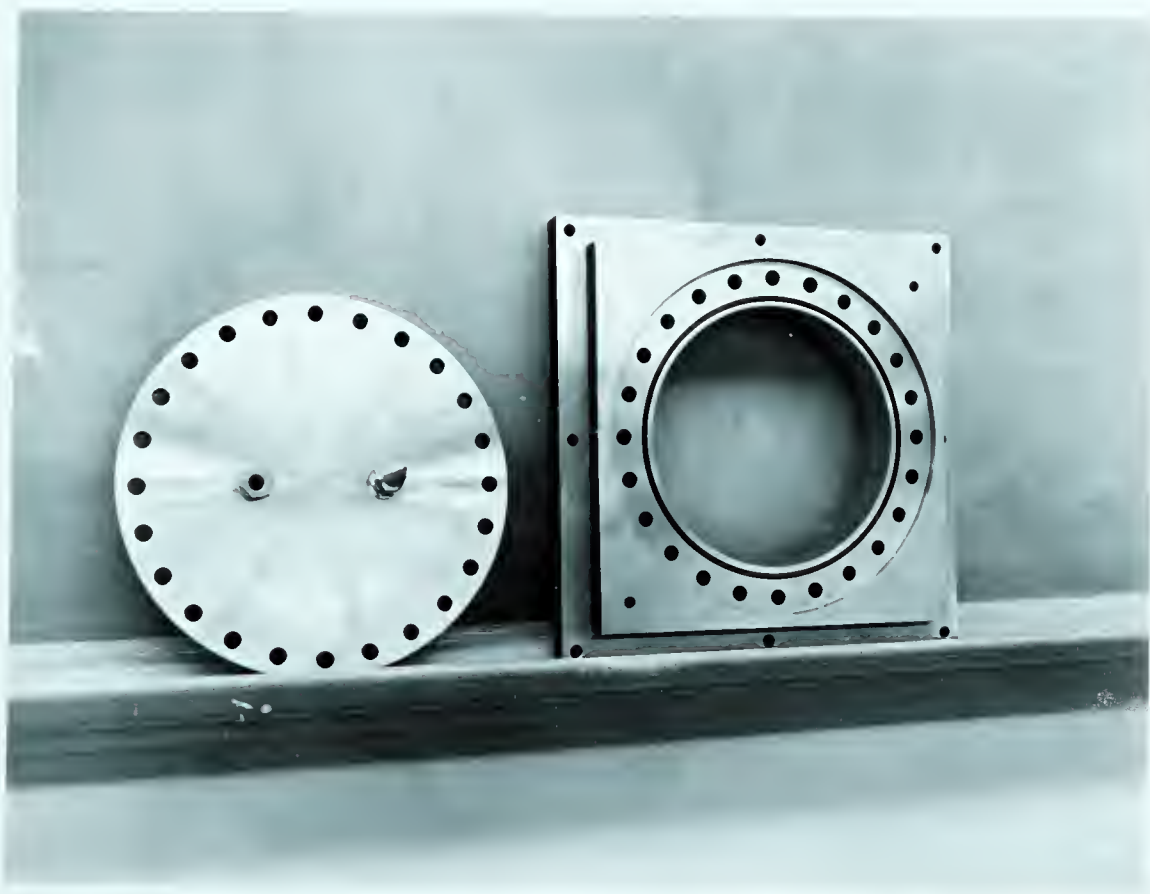


Fig. 25. Support for circular clamped plate. Both concentrated load and uniformly distributed load can be applied.



for aluminum,  $D_C = 247$  (load  $P = 2.377$  lb.) was obtained by using  $\mu = 0.30$ . The value of  $D_C$  ( $= 242$  lb-in.) for aluminum plate found by using a circular clamped plate with concentrated centre load was in good agreement with that found by using a square plate.

#### 4. Test procedure.

In order to ensure that the deflection of the plate does not exceed one-half the plate thickness, a deflection - load diagram (Fig. 26) was first plotted by loading the model gradually and measuring the corresponding deflection by a dial indicator. From Fig. 26, loads were chosen so as to keep deflections of the model plate less than one-half of the plate thickness.

In each test, the first exposure was taken with a small initial load on the model, and the second exposure was then taken after application of desired load. After taking the first picture, the grid was rotated through 90 degrees, and the fringe pattern for the other direction was made. Analysis was made upon the enlargements of these two negatives.

#### 5. Reduction of data.

In reducing the data from the fringe patterns to determine the curvatures and twists, the following procedure was followed:

Enlargements. The photographs were first enlarged to full scale. The chief quality aimed for was maximum contrast between the even fringes and the half fringes as well as sharpness of detail. Kodak Kodabromide, light weight, A.5, 11 x 14 in.



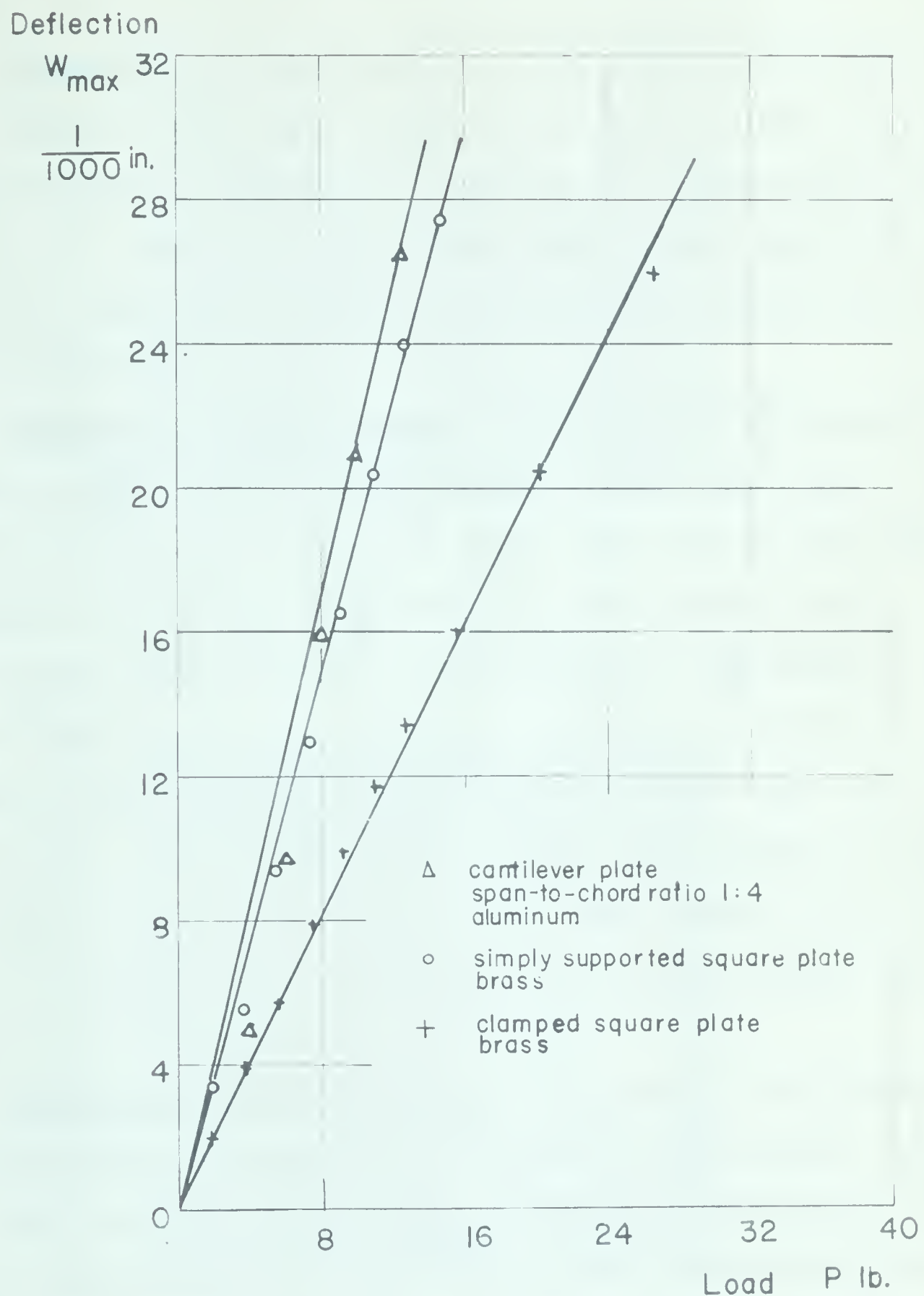


Fig. 26. Relation between deflection and load.



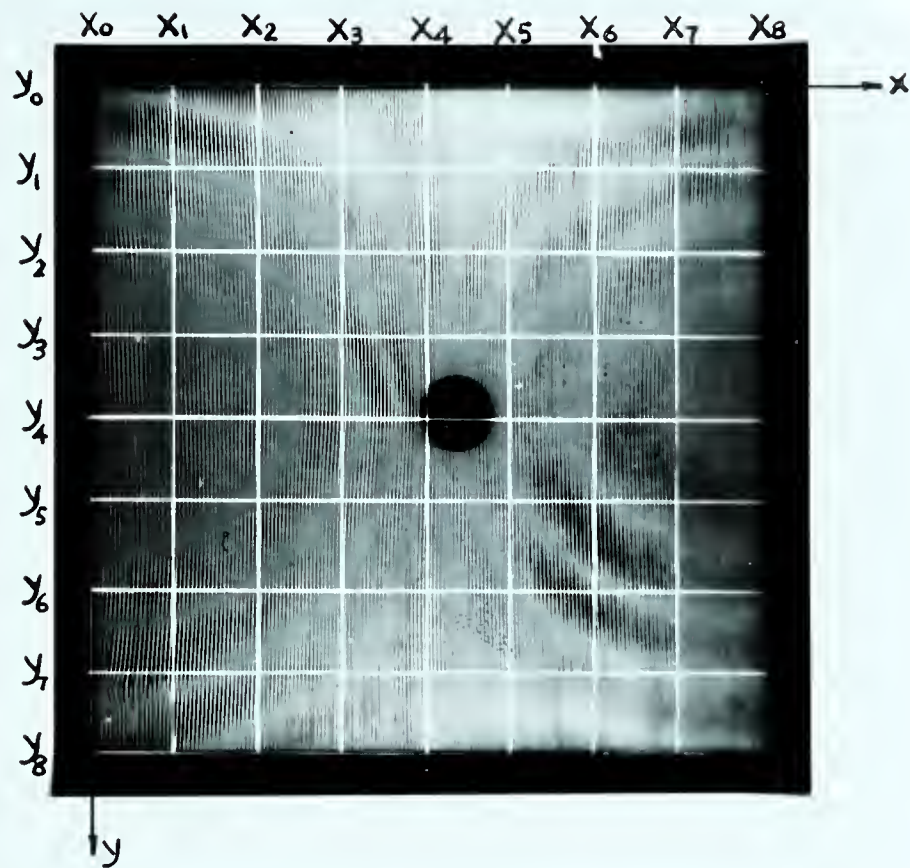
photographic paper was found to be satisfactory for this purpose.

Preparation of the picture. Next, grid lines with spacing  $\frac{a}{8}$ , where  $a$  is the side length of the square plate, were drawn directly on the photograph, and then the fringes were numbered (Fig. 27). Each half fringe was then traced, and each point where it intersected with a grid line was marked with a very small pin-hole.

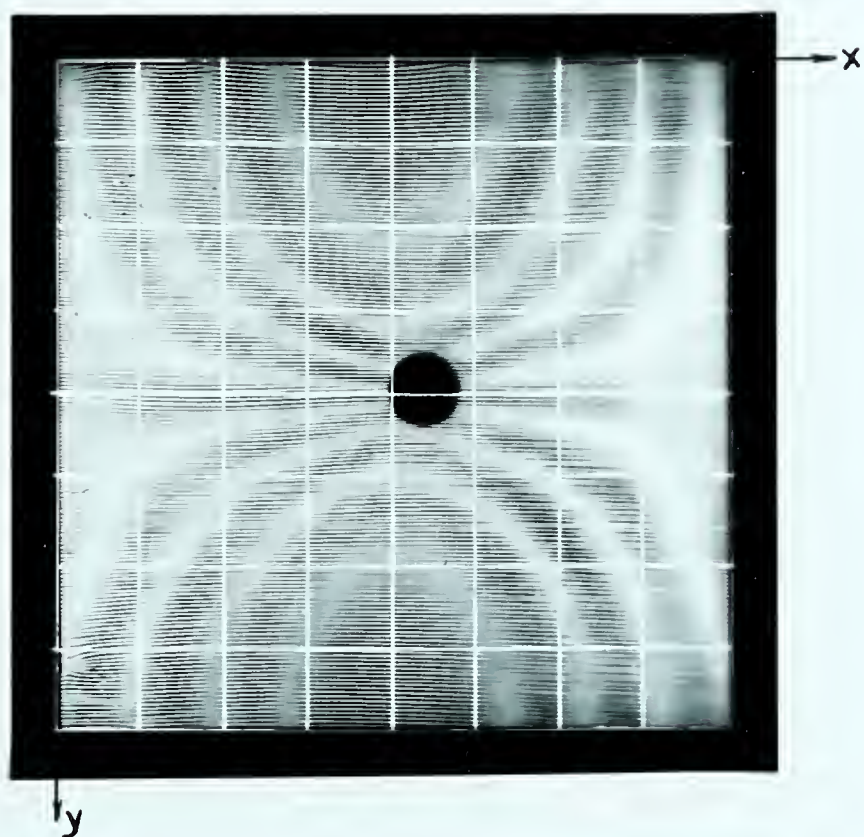
Drawing the slope curves. The curves of  $\frac{\partial w}{\partial x}$  versus  $x$ ,  $\frac{\partial w}{\partial x}$  versus  $y$ ,  $\frac{\partial w}{\partial y}$  versus  $y$ , and  $\frac{\partial w}{\partial y}$  versus  $x$  were next drawn. First, each half fringe was located along each line of the grid. For example, the curves of  $\frac{\partial w}{\partial x}$  versus  $x$  along grid lines  $y_1$ ,  $y_2$ ,  $y_3$ , and  $y_4$  are shown in Fig. 28, the curves of  $\frac{\partial w}{\partial x}$  versus  $y$  along grid lines  $x_0$ ,  $x_1$ ,  $x_2$ , and  $x_3$ , are shown in Fig. 29. In drawing these curves, it was helpful to draw both sets simultaneously, for the results of one set was helpful in locating points on the curves of the other. For example, the value of  $\frac{\partial w}{\partial x}$  at  $x_1$  on the curve  $y_1$  in Fig. 28 is equal to the value of  $\frac{\partial w}{\partial x}$  at  $y_1$  on the curve  $x_1$  in Fig. 29.

Determination of curvatures. In general, the curvature  $\frac{\partial^2 w}{\partial x^2}$  was found by measuring the slope of the curves, such as in Fig. 28, and the twist  $\frac{\partial^2 w}{\partial x \partial y}$  by finding the slope of the curve as in Fig. 29. These slopes were approximated at a point by laying a straight edge such that it intersected the curve at two points equidistant on either side of the point.





a) For slope in x-direction.



b) For slope in y-direction.

Fig. 27. Fringe patterns for simply supported square plate with concentrated centre load. Initial load=2.25 lb. final load  $P=14.78$  lb. Brass sheet thickness=.0641 in.



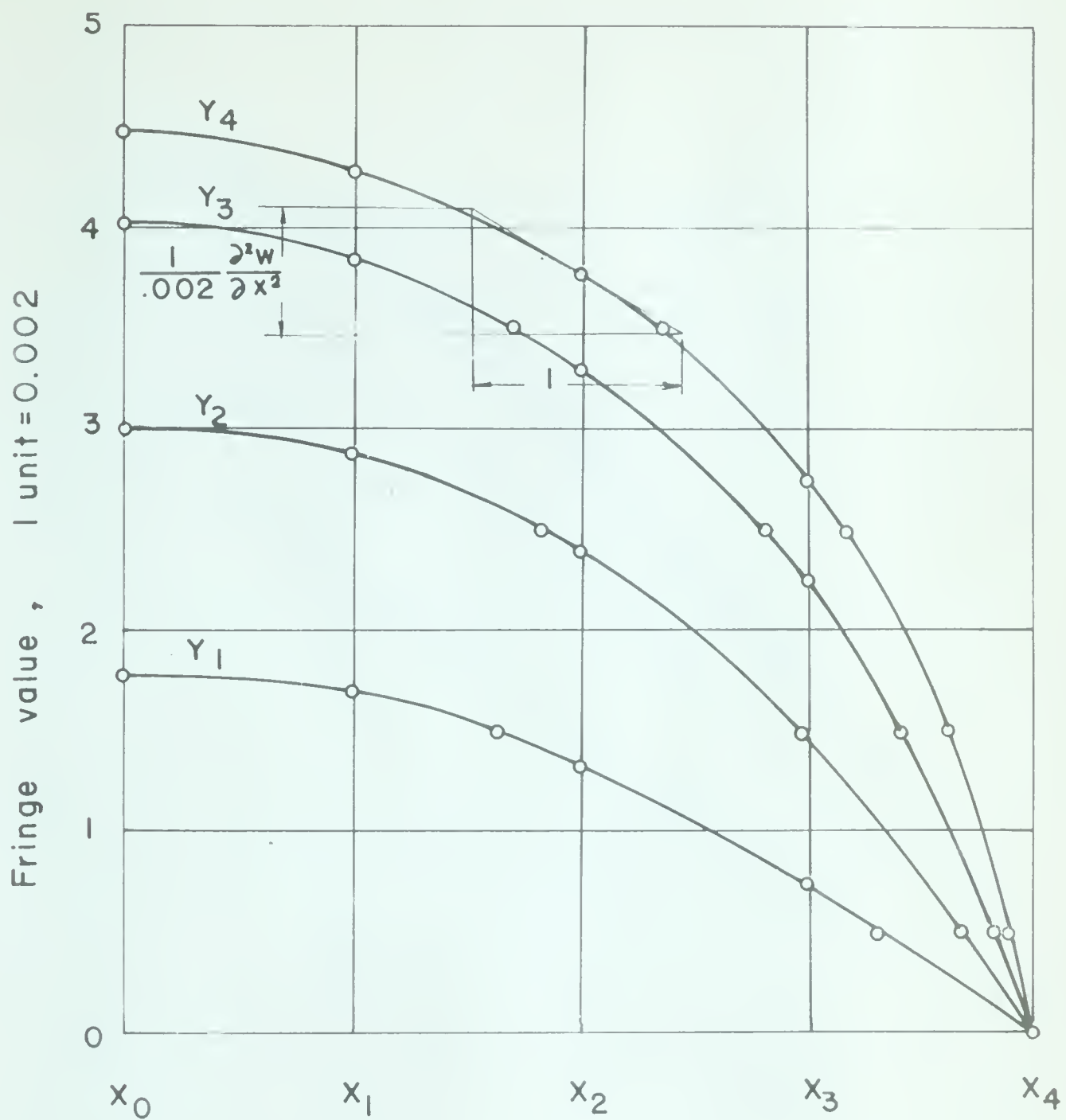


Fig.28. Plot of  $\frac{\partial w}{\partial x}$  fringe values against  $x$   
along  $y_1, y_2, y_3$ , and  $y_4$ .



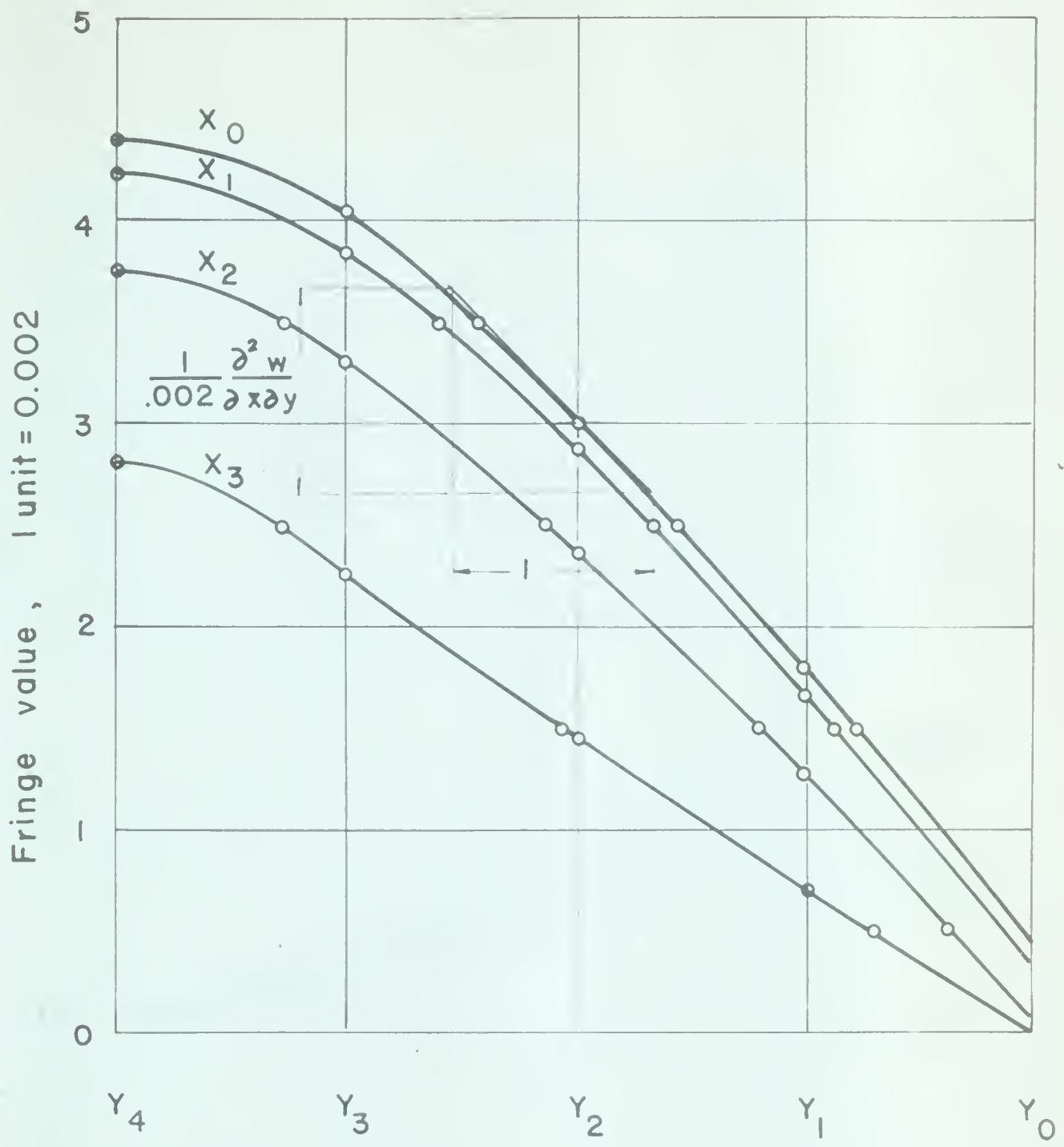


Fig. 29. Plot of  $\frac{\partial w}{\partial x}$  fringe values against  $y$   
along  $x_0, x_1, x_2$ , and  $x_3$ .



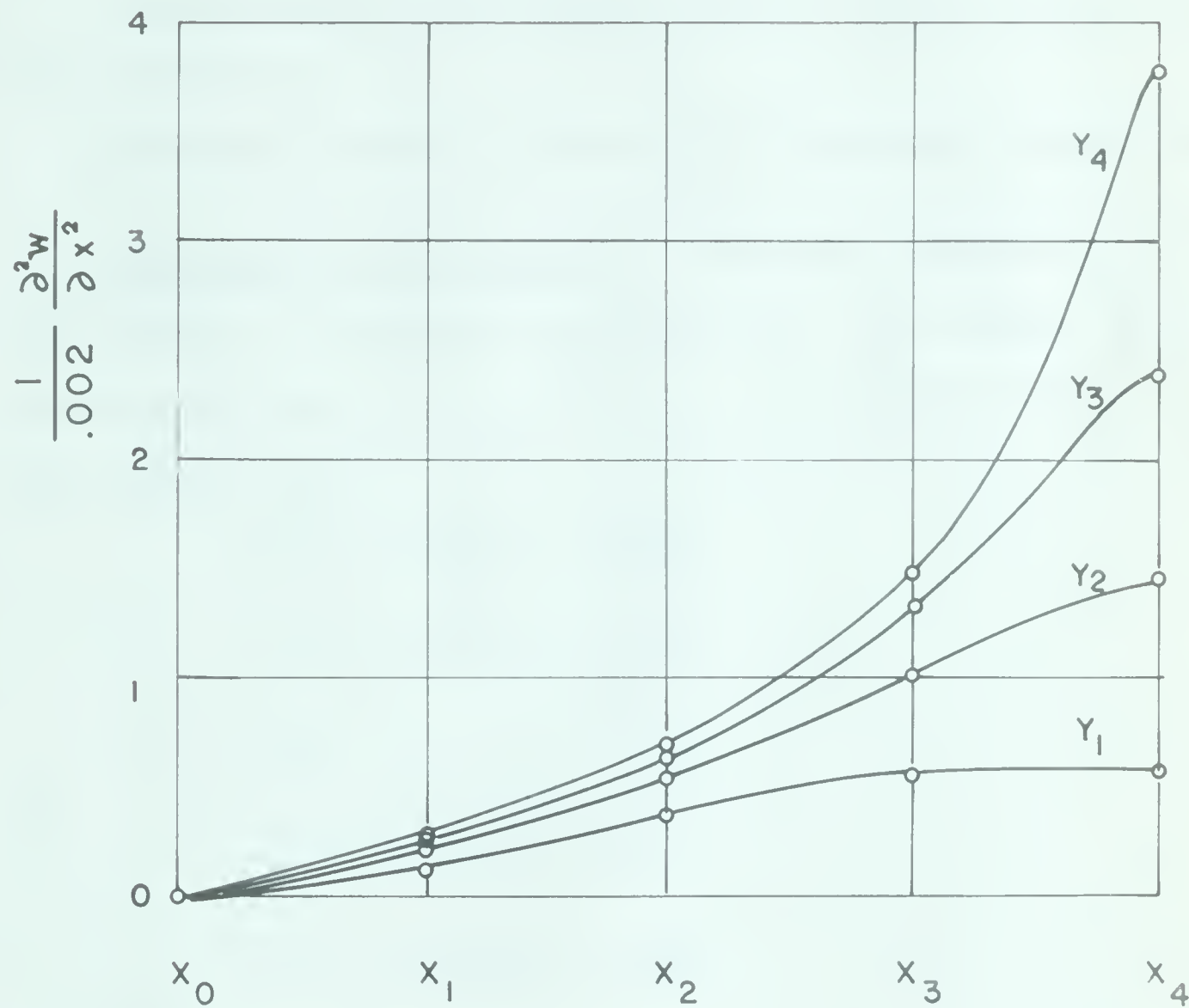


Fig. 30. Plot of  $\frac{\partial^2 w}{\partial x^2}$  value against  $x$ .



In finding the curvature at the edge, the values were extrapolated by finding the curvatures at several points approaching the edge and connecting them by a curve (2).

The condition that bending moments along the free edge are zero requires

Curvature normal to edge  $= -(\mu)$  (curvature tangent to the edge)

Determination of moments. After the curvatures and twists are found, all data are available for the moment determinations. From equations 2, 3, and 4, the bending moments and twisting moments are:

$$M_x = -D \left( \frac{\partial^2 w}{\partial x^2} + \mu \frac{\partial^2 w}{\partial y^2} \right)$$

$$M_y = -D \left( \frac{\partial^2 w}{\partial y^2} + \mu \frac{\partial^2 w}{\partial x^2} \right)$$

$$M_{xy} = -D (1-\mu) \left( \frac{\partial^2 w}{\partial x \partial y} \right)$$

or  $\frac{M_x}{P} = -\frac{D}{P} \left( \frac{\partial^2 w}{\partial x^2} + \mu \frac{\partial^2 w}{\partial y^2} \right)$

$$\frac{M_y}{P} = -\frac{D}{P} \left( \frac{\partial^2 w}{\partial y^2} + \mu \frac{\partial^2 w}{\partial x^2} \right)$$

$$\frac{M_{xy}}{P} = -\frac{D}{P} (1-\mu) \left( \frac{\partial^2 w}{\partial x \partial y} \right).$$



#### IV. COMPARISONS OF EXPERIMENTAL RESULTS WITH ANALYTICAL RESULTS

##### 1. Test results.

Simply supported square plate. The fringe patterns for a simply supported square plate subjected to concentrated centre load are shown in Fig. 27. The distribution of bending moments and twisting moments along each grid line is represented graphically in Fig. 31, and Fig. 32. Numerical values are tabulated in Table 2.

Clamped square plate. Fig. 33 shows the fringe patterns for the clamped square plate with concentrated centre load. The distribution of  $M_x$ ,  $M_y$ , and  $M_{xy}$  is shown in Fig. 34, and Fig. 35. Numerical values are given in Table 3.

Cantilever plate. Fig. 13 shows the fringe patterns for the cantilever plate with concentrated load applied opposite the clamped edge. Graphical representation of  $M_x$ ,  $M_y$  is shown in Fig. 37. Numerical values of  $M_x$ ,  $M_y$  and  $w$  are given in Table 4. Also, deflection profiles of this plate are shown in Fig. 36.

##### 2. Comparisons of the results.

Simply supported square plate. Both experimental and theoretical results for the simply supported square plate with concentrated centre load are given in the following table:



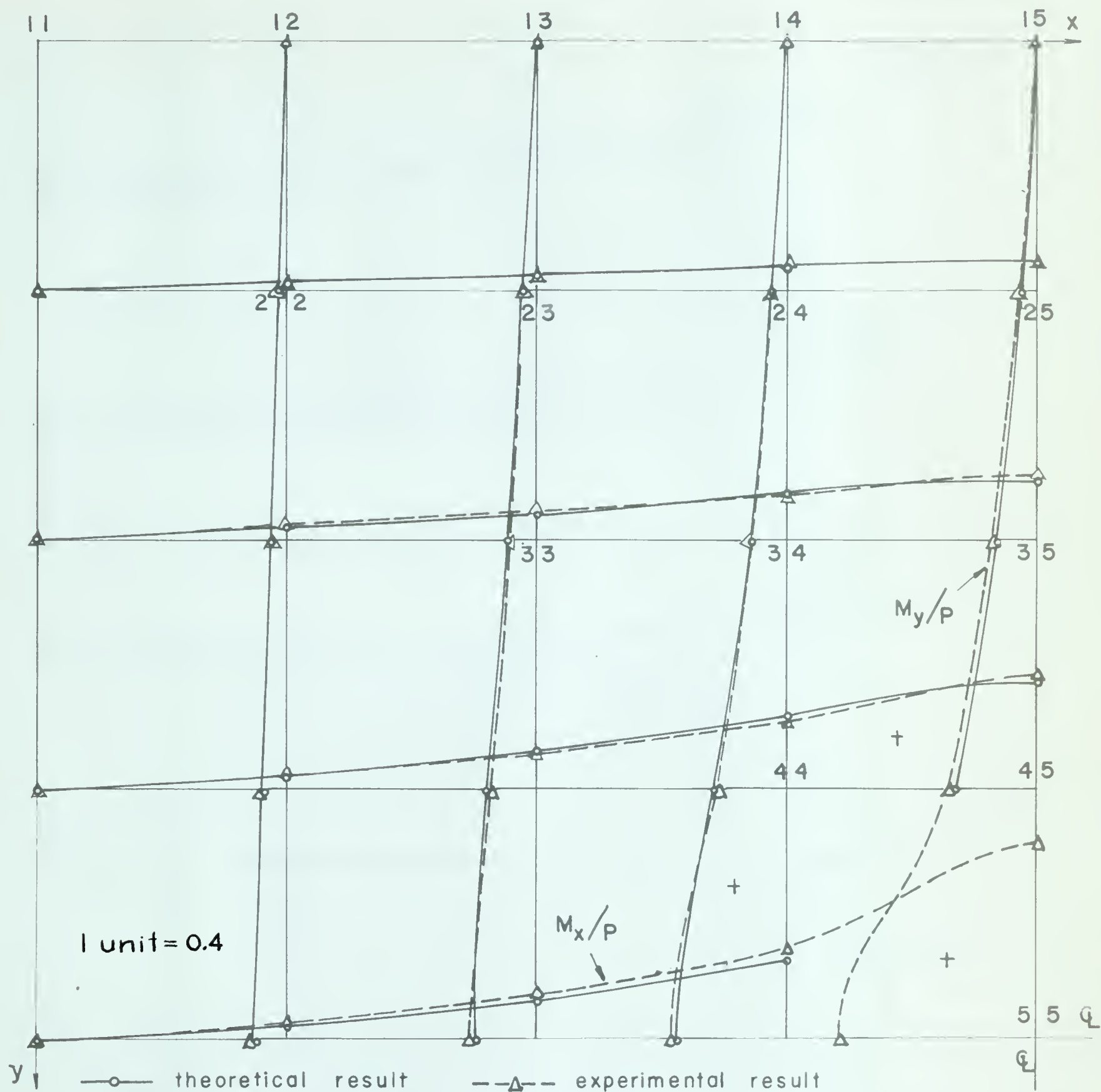


Fig.31. Distribution of  $M_x/P$ ,  $M_y/P$  for simply supported square plate with concentrated centre load.  $P=14.78$  lb. Brass.

Max. theoretical deflection at centre:  $w = \frac{0.0116Pa^4}{D}$

Max. experimental deflection at centre:  $w = \frac{0.01118Pa^4}{D}$



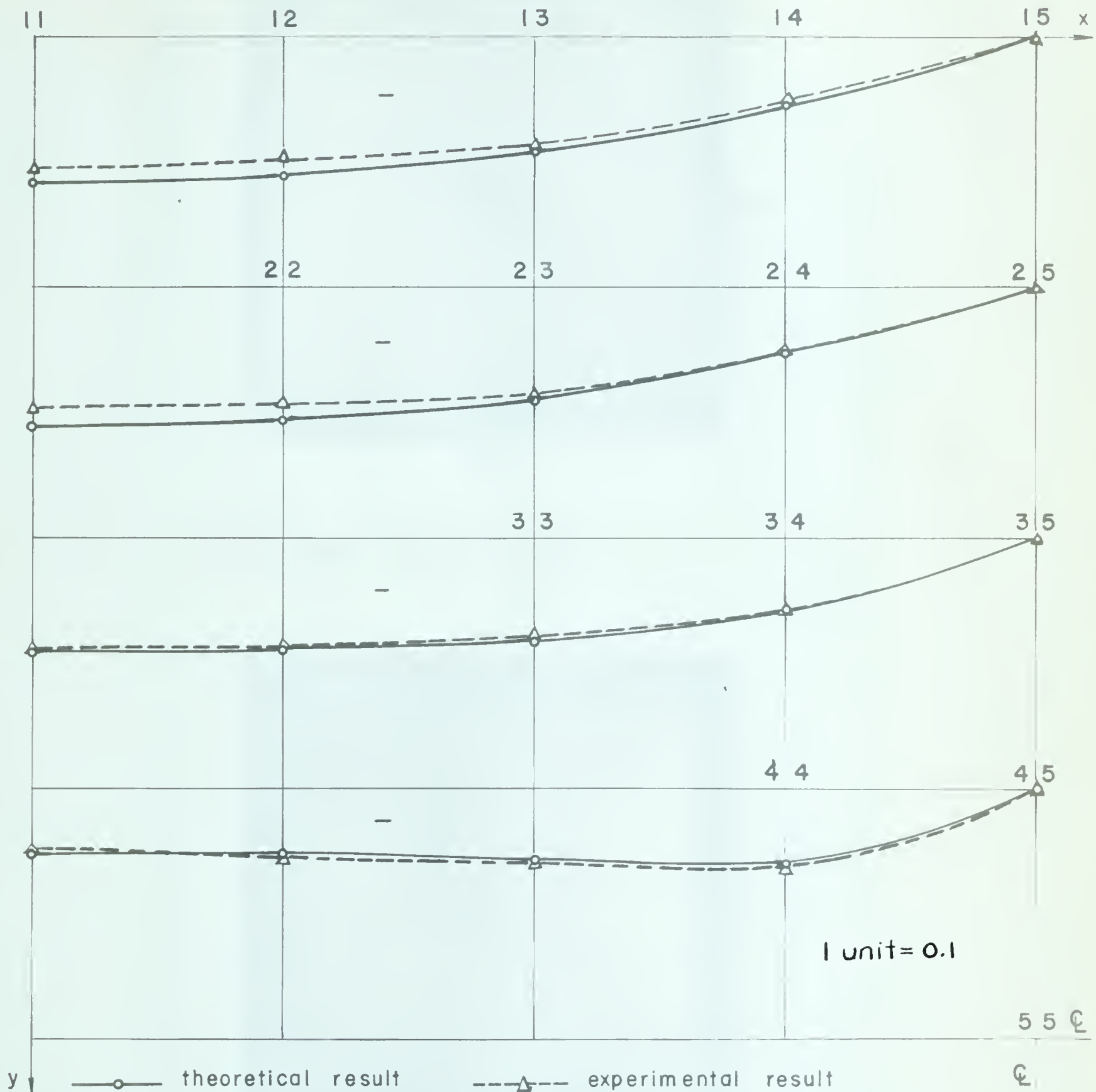
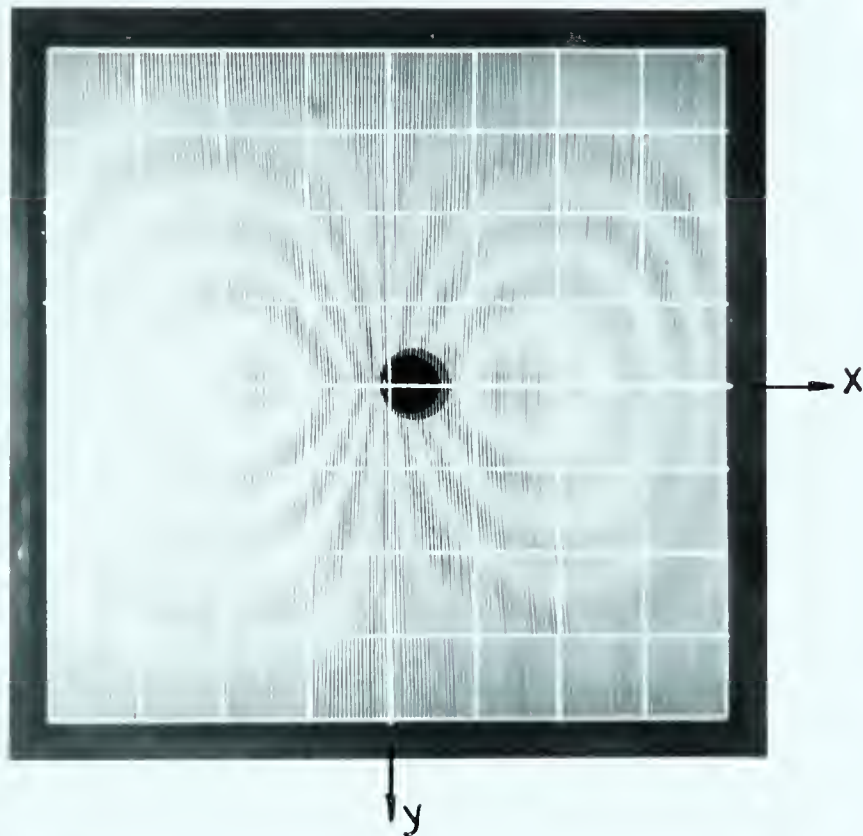
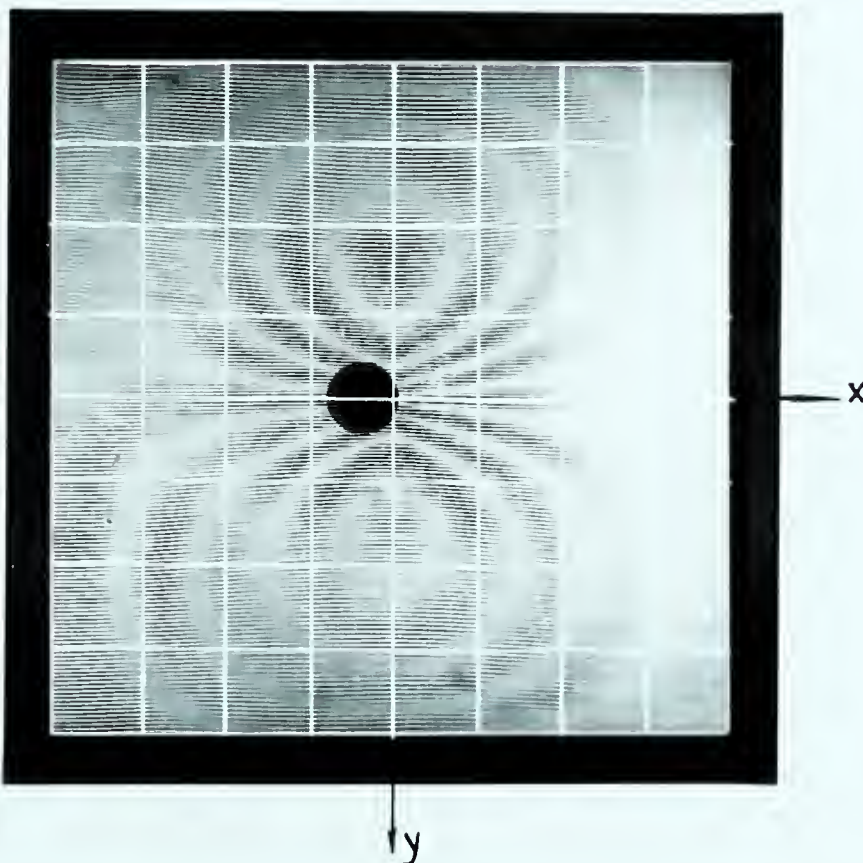


Fig.32. Distribution of  $M_{xy}/P$  for simply supported square plate with concentrated centre load.  $P=14.78$  lb. Brass.





a) For slope in x-direction.



b) For slope in y-direction.

Fig. 33. Fringe patterns for clamped square plate with concentrated centre load. Load  $P=27.52$  lb.  
Brass sheet thickness=.0641 in.



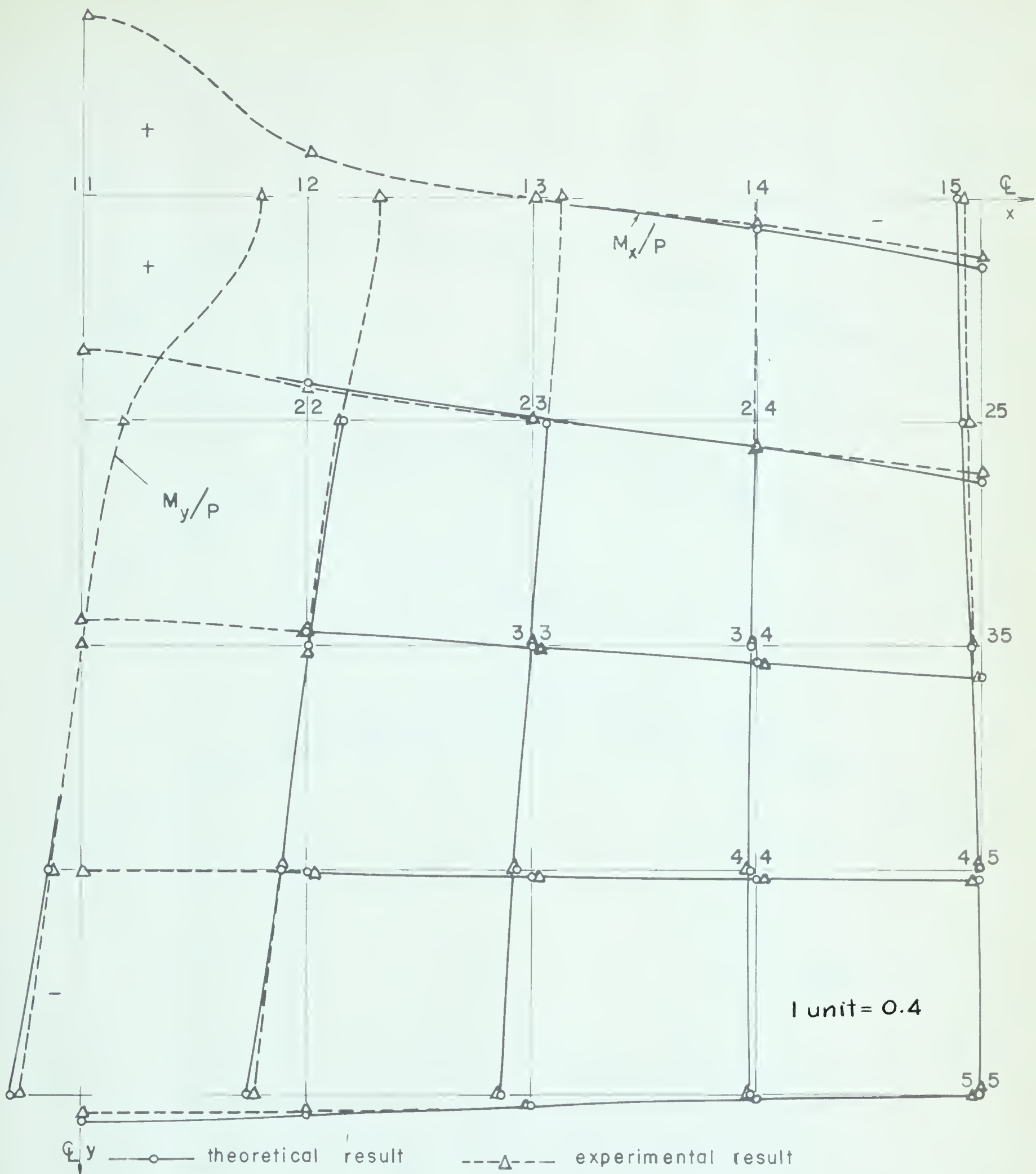


Fig.34. Distribution of  $M_x/P$ ,  $M_y/P$  for clamped square plate with concentrated centre load.  $P=27.52$  lb. Brass.

Max. theoretical deflection at centre:  $w=0.00560P^4/D$

Max. experimental deflection at centre:  $w=0.00527P^4/D$



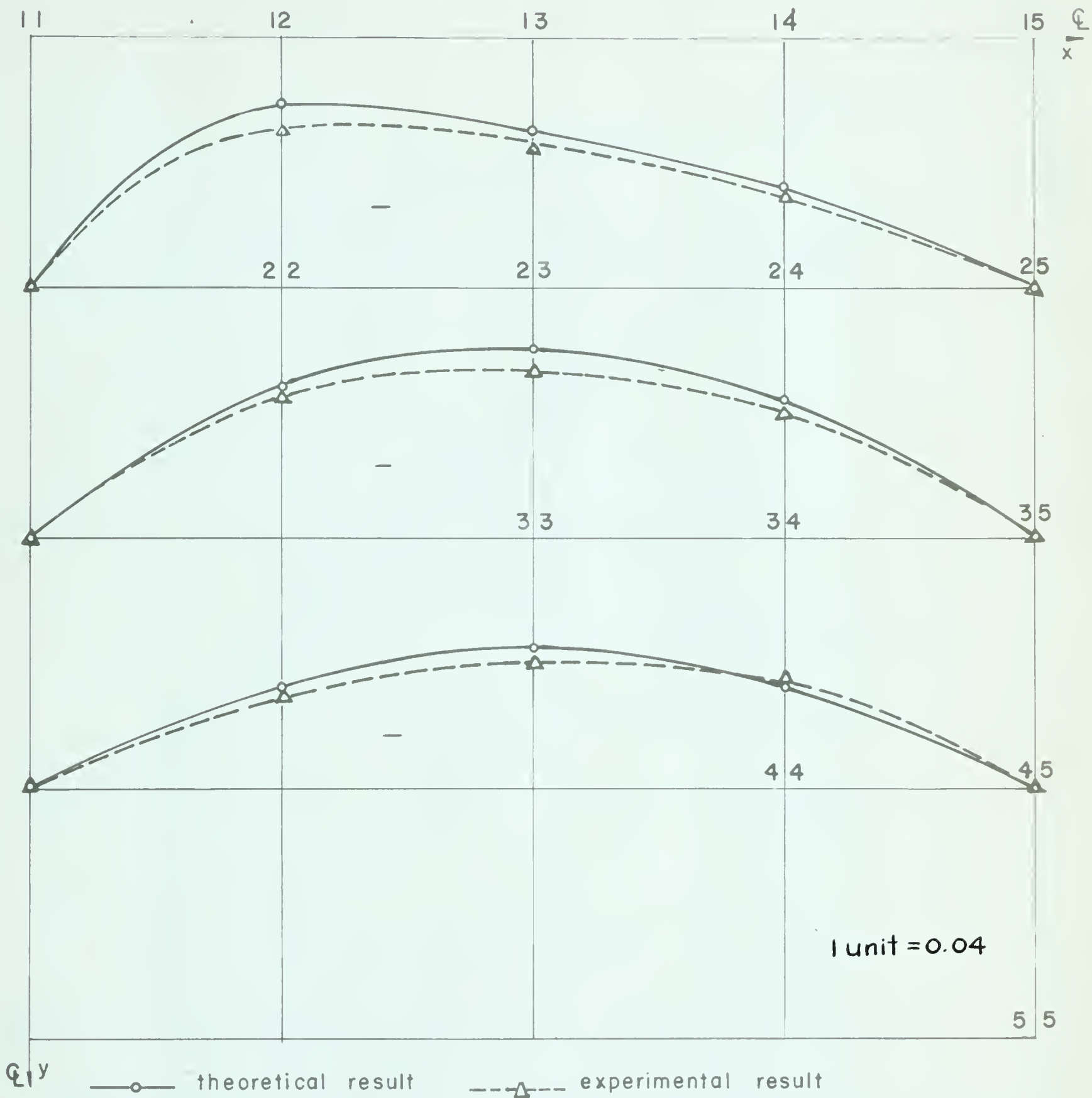


Fig.35. Distribution of  $M_{xy}/P$  for clamped square plate with concentrated centre load.  $P = 27.52$  lb. Brass.



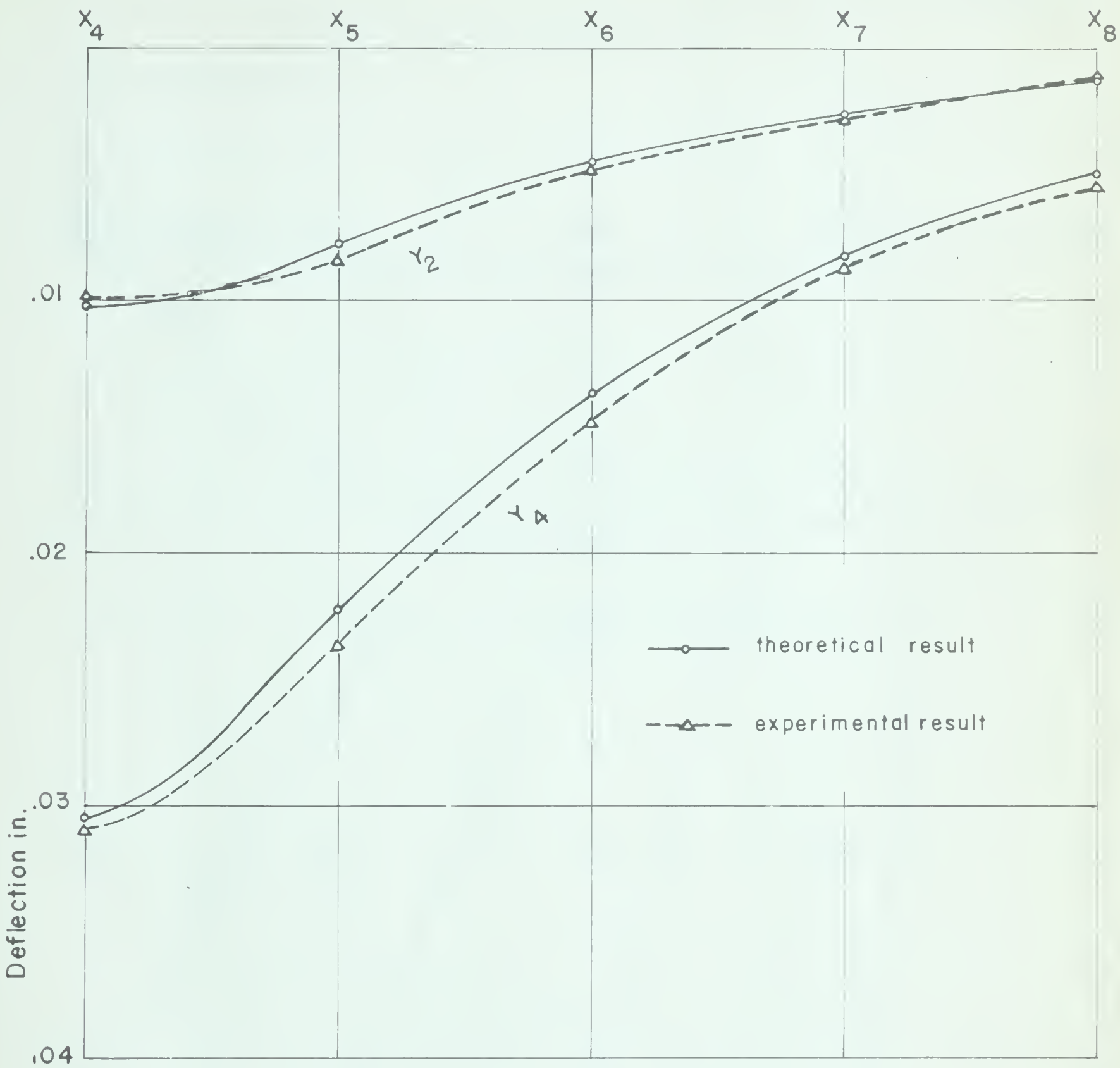


Fig.36. Deflection profiles for cantilever plate with concentrated load  $P=10.019$  lb. applied at point 31.

Max. theoretical deflection at point 31:  $w=0.18773 P a^4 / D$

Max. experimental deflection at point 31:  $w=0.19040 P a^4 / D$



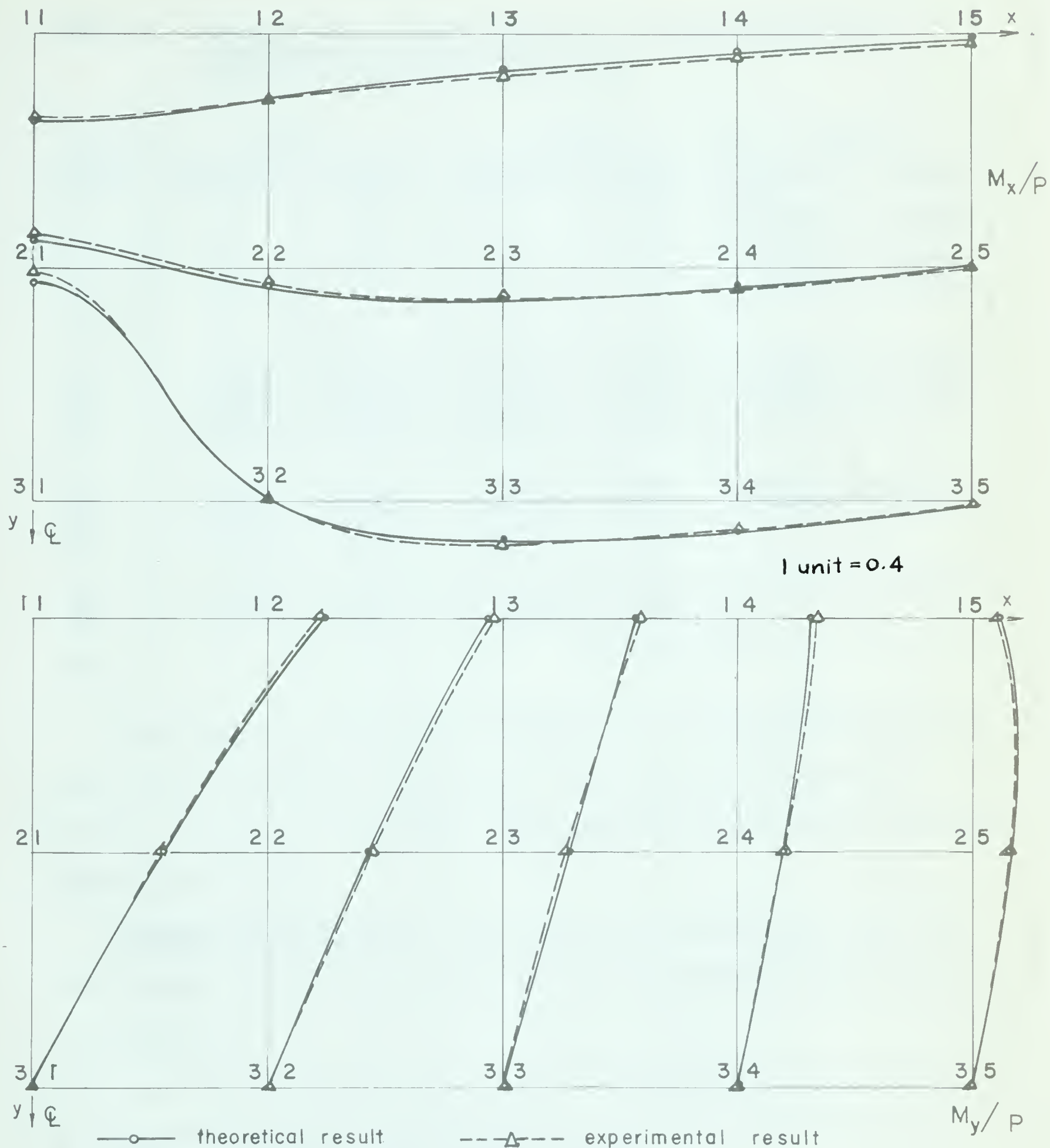


Fig.37. Distribution of  $M_x/P$ ,  $M_y/P$  for cantilever plate with concentrated load  $P=10.019$  lb. applied at point 31.  
span-to-chord ratio = 1:4, Aluminum.



TABLE 2. MOMENTS IN A SIMPLY SUPPORTED SQUARE PLATE WITH CONCENTRATED CENTRE LOAD.  
POISSON'S RATIO = 0.33 (BRASS)

NET POINT	$M_x/P$		$M_y/P$		$M_{xy}/P$	
	Navier	Moire	Navier	Moire	Navier	Moire
11	0	0	0	0	-.05840	-.05260
12	0	0	0	0	-.05540	-.04836
13	0	0	0	0	-.04530	-.04497
14	0	0	0	0	-.02630	-.02545
15	0	0	0	0	0	0
22	.01140	.01115	.01140	.01158	-.05300	-.04666
23	.02490	.02783	.02030	.02102	-.04460	-.04369
24	.03920	.04154	.02470	.02837	-.02690	-.02757
25	.04610#	.04237	.02620#	.02922	0	0
33	.04660	.04654	.04660	.04527	-.04100	-.03818
34	.08000#	.07840	.05950#	.05973	-.02900	-.02969
35	.09990#	.10626	.06240#	.07232	0	0
44	.11800	.11054	.11800#	.11266	-.03000	-.03182
45	.17700	.18292	.13000#	.14388	0	0
55	*	.31922	*	.31922	0	0

Observing this table the maximum error is approximately 16 per cent at net point 35 for  $M_y$ . The maximum deflection at centre is  $w_{max} = 0.01118 \frac{Pa^2}{D}$ , approximately 4 per cent less than theoretical result.

Clamped square plate. Experimental results were compared with Young's result (7). The result of calculation is given in Table 3.

\* Series diverges at this point.

# Series converges slowly at this point.

+ For net points see Fig. 2.



TABLE 3. MOMENTS IN A CLAMPED SQUARE PLATE WITH CONCENTRATED CENTRE LOAD. POISSON'S RATIO = 0.33  
MATERIAL: BRASS,

NET POINTS	$M_x/P$		$M_y/P$		$M_{xy}/P$	
	Young	Moire	Young	Moire	Young	Moire
11	*	.31665	*	.31665	0	0
12	#	.07364	#	.12125	0	0
13	#	-.00204	#	.04420	0	0
14	-.05100	-.05077	-.00200	-.00221	0	0
15	-.12500	-.10986	-.04100	-.04622	0	0
22	.06300	.05816	.06300	.05986	-.02910	-.02506
23	#	.00374	.02976	.02976	-.02460	-.02210
24	-.04500	-.04677	-.00540	-.00476	-.01630	-.01481
25	-.10500	-.09098	-.03400	-.02993	0	0
33	-.00196	-.00181	-.00196	-.00181	-.03016	-.02688
34	-.03000	-.03163	-.01000	-.01037	-.02237	-.02005
35	-.05700	-.05782	-.01890	-.01900	0	0
44	-.01480	-.01497	-.01480	-.01497	-.01637	-.01731
45	-.01080	-.11900	-.00360	-.00393	0	0
55	0	0	0	0	0	0

By comparing the results from table 3, the maximum error is also 16 per cent at net point 25 for  $M_y$ . Maximum deflection at the centre of the plate is  $w_{max} = 0.00527 \frac{Pa^2}{D}$ , it yields 6 per cent less than obtained by Young.

Cantilever plate. The finite cantilever plate subjected to a transverse loading is one problem for which an exact solution has not been achieved. However, Holl's (10) finite-difference solution provides a check for this case.

\* Series diverges at this point.

# Series converges slowly at this point.

+ For net points see Fig. 3.



Regarding the accuracy obtainable, it is observed that maximum deviation is about 20 per cent at net point 21 for  $M_x$ , and 18 per cent at net point 11 for  $w$ . Values of bending moments and deflections are given in Table 4.

In comparing the results, it is to be noted that Holl's solution is an approximate solution.

TABLE 4. MOMENTS AND DEFLECTIONS FOR A CANTILEVER PLATE WITH A CONCENTRATED EDGE LOAD AT THE MID-POINT OF THE FREE EDGE. POISSON'S RATIO = 0.30 MATERIAL: ALUMINUM. SPAN-CHORD-RATIO = 1:4

NET <sup>+</sup> POINTS	$M_x/P$		$M_y/P$		$w/\frac{Pa^2}{D}$	
	Holl	Moire	Holl	Moire	Holl	Moire
11	-.14902	-.14640	-.49672	-.48807	0	0
12	-.11206	-.11512	-.37352	-.38405	0	0
13	-.06802	-.07149	-.22672	-.23861	0	0
14	-.03780	-.04067	-.12600	-.13558	0	0
15	-.01498	-.01430	-.04992	-.04733	0	0
21	+.04696	+.05620	-.21714	-.21643	.01006	.00996
22	-.03931	-.03352	-.16670	-.17156	.00756	.00843
23	-.05539	-.05423	-.11477	-.10600	.00459	.00478
24	-.03444	-.03796	-.07780	-.07592	.00255	.00276
25	0	0	-.06432	-.06089	.00101	.00119
31	+.37703	+.39711	0	0	.03041	.03090
32	+.00186	+.00197	0	0	.022022	.02360
33	-.06766	-.07420	0	0	.01355	.01473
34	-.05070	-.04856	0	0	.00809	.00860
35	0	0	0	0	.00488	.00548

The maximum experimental deflection is  $w_{max} = 0.1904 \frac{Pa^2}{D}$  which is 1.59 per cent greater than that given by Holl's solution.

+ For net points see Fig. 4.



## V. DISCUSSIONS AND CONCLUSIONS

The use of plastic materials for the Moiré Method was well described by Ligtenberg and Bradley. One of the disadvantages of using plastic materials is that the modulus of elasticity varies with humidity and temperature. This will be an obstacle in applying Moiré method to some other plate problems, for example, thermal stresses in plates. Since the values of moduli of elasticity for metals may be considered as constant for practical purposes, it is possible to take advantage of this property. And once the material is calibrated, there is no need to repeat calibrating for the same kind of material in other test. In such case, much labour can be saved during each test. Therefore, the use of metal models is also particularly attractive from the standpoint of saving time.

In applying the Moiré method, several possible sources of errors may be listed as follows:

- a. Membrane action of the plate due to large deflection.

According to Sturm and Moore's experimental result (9), for plates in which the deflection does not exceed one half the thickness of the plate, less than 5 per cent of the load may be assumed to be carried by membrane force.

- b. Due to calibration, The value of D found by using a square calibration plate with a concentrated load  $p = 2.377 \text{ lb.}$  at one corner was  $D_c = 247 \text{ lb-in.}$ ; by



using a circular clamped plate with a concentrated load  $P = 14$  lb. at the centre of the plate,  $D_C = 242$  lb-in; for a circular clamped plate with uniformly distributed load  $q = 1.083 \frac{\text{lb}}{\text{in}^2}$ ,  $D_C = 239$  lb-in. The maximum error is approximately 5 per cent.

- c. Due to the use of the incorrect value of Poisson's ratio for the particular plate tested. For example, if  $\mu$  is taken as 0.32 instead of 0.33, the maximum difference for moments by using  $\mu = 0.32$  was 11 per cent greater than using  $\mu = 0.33$ .
- d. Due to experimental errors in the measurement of load-- it is estimated as about 1 per cent.
- e. Due to reduction of data--it may be as great as 4 per cent.
- f. Due to possible imperfect realization of a boundary condition.
- g. Due to shear deflection not accounted for in the theory.

As Ligtenberg (1) pointed out, accurate results are impossible near a point load. This is caused in part by the fact that the theory is applicable to the middle plane of the plate, whereas measurements are taken from the surface. Furthermore, even the elementary theory is not applicable near a concentrated load because the stresses normal to the plane of the plate cannot be assumed to be zero. Observing table 2, and 3, the series for bending moments do not converge well along the



centre line of the simply supported square plate and the clamped square plate, and diverge at the centre of each plate.

Shearing forces  $Q_x$  and  $Q_y$  are obtained from the third derivatives of the deflections. It was found that the values of  $\frac{\partial^3 w}{\partial x^3}$ , and  $\frac{\partial^3 w}{\partial x \partial y^2}$  cannot be measured with sufficient accuracy by the Moiré method.

In comparing experimental results with theoretical results, it is observed that the maximum error is 16 per cent for the bending moment, and 14 per cent for the twisting moment in the cases of simply supported square plate and the clamped square plate; for the cantilever plate, 20 per cent deviation was observed for  $M_x$ , about 10 per cent for  $M_y$ , and about 18 per cent for deflection. It is of interest to note that the finite elements are used in the formation of difference equation networks. Consequently, the results obtained are only approximate. This approximation can be improved as the elements become smaller. For the case of cantilever plate, the accuracy cannot be stated exactly.

Moiré method yields approximate solution to laterally loaded plate problems with complicated boundary conditions. From the viewpoint of engineering application, the Moiré method is believed to be a useful tool for obtaining valuable informations concerning bending moments, twisting moments, and deflections in bending of plates with complicated boundary conditions.

Among the problems of bending of plates, those which might be studied effectively by the Moiré method are:



- a. Thermal stresses in plates--since the modulus of elasticity may be assumed as constant within certain range of temperature, it is possible to take advantage of this particular property to apply Moiré method to thermal stress problems in thin plates. Preliminary investigation shows that Moiré method can be applied to thermal stress analysis.
- b. Moments and deflections in some elastically supported plate problems.
- c. Study of plates with stiffeners.
- d. Plates with variable thickness.

It is believed that the Moiré method would offer useful results in these studies and would provide valuable informations for application in practical designs.



APPENDIX. COMPUTER PROGRAMS AND DATA

1. Simply supported square plate with concentrated centre load.



```

••I MECH. ENG. H. R. T. O. 923114
  DIMENSION A(20,20),B(20,20),C(20,20)
1  READ 2,I,IX,JY,U
2  FORMAT(3I5,F10.5)
  PUNCH 5
5  FORMAT(2X2HMN,4X1HL,4X1HK,10X3HTXM,17X3HTYM,17X4HTXYM//)
  DO 30 K=1,JY
  DO 30 L=K,IX
  DO 10 TM=1,I
  M=2*I-1
  AM=M
  RL=L-1
  PSM=SINF(AM*1.570795)
  RUM=AM*RL*0.392699
  QSM=SINF(RUM)
  COM=COSF(RUM)
  DO 10 TN=1,T
  N=2*TN-1
  AN=N
  CK=K-1
  PSN=SINF(AN*1.570795)
  RUN=AN*CK*0.392699
  QSN=SINF(RUN)
  CON=COSF(RUN)
  DMN=(AM*AM+AN*AN)**2
  ZM=AM*AM+U*AN*AN
  ZN=AN*AN+U*AM*AM
  PMN=ZM/DMN
  SMN=ZN/DMN
  TMN=AM*AN/DMN
  RSMN=PSM*PSN
  DSMN=QSM*QSN
  GSMN=COM*CON
  XM=PMN*PSMN*DSMN
  YM=SMN*PSMN*DSMN
  XYM=TMN*RSMN*GSMN
  A(IN,IM)=XM
  B(IN,IM)=YM
10  C(IN,IM)=XYM
  SUXM=0.0
  SUYM=0.0
  SUXYM=1.0
  MN=1
15  DO 20 TM=1,MN
  DO 20 TN=1,MN
  SUXM=SUXM+A(IN,IM)
  SUYM=SUYM+B(IN,IM)
20  SUXYM=SUXYM+C(IN,IM)
  BB=4.0/3.14159**2
  BRUU=BB*(1.0-U)
  TXM=BR*SUXM
  TYM=BB*SUYM
  TXYM=-BRUU*SUXYM
  PUNCH 6,MN,L,K,TXM,TYM,TXYM
  FORMAT(3I5,2F20.8)
6   IF(MN-1)14,30,30
14  MN=MN+1
  TXM=0.0
  TYM=0.0
  TXYM=0.0
  SUXM=0.0

```



SYM=0.0  
SUXYM=0.0  
GO TO 15  
30 CONTINUE  
GO TO 1  
END

15 5 5 0.34















1	4	4	• 115 26 1 + .	• 115 26 1 + .	• 115 26 1 + .	• 115 26 1 + .
2	4	4	• 13627288E+00	• 13627288E+00	• 13627288E+00	• 13627288E+00
3	4	4	• 12741064E+00	• 12741064E+00	• 12741064E+00	• 12741064E+00
4	4	4	• 11984685E+00	• 11984685E+00	• 11984685E+00	• 11984685E+00
5	4	4	• 11887457E+00	• 11887457E+00	• 11887457E+00	• 11887457E+00
6	4	4	• 11947349E+00	• 11947349E+00	• 11947349E+00	• 11947349E+00
7	4	4	• 11883118E+00	• 11883118E+00	• 11883118E+00	• 11883118E+00
8	4	4	• 11818849E+00	• 11818849E+00	• 11818849E+00	• 11818849E+00
9	4	4	• 11844729E+00	• 11844729E+00	• 11844729E+00	• 11844729E+00
10	4	4	• 11874483E+00	• 11874483E+00	• 11874483E+00	• 11874483E+00
11	4	4	• 11847183E+00	• 11847183E+00	• 11847183E+00	• 11847183E+00
12	4	4	• 11819155E+00	• 11819155E+00	• 11819155E+00	• 11819155E+00
13	4	4	• 11832265E+00	• 11832265E+00	• 11832265E+00	• 11832265E+00
14	4	4	• 11847125E+00	• 11847125E+00	• 11847125E+00	• 11847125E+00
15	4	4	• 11832255E+00	• 11832255E+00	• 11832255E+00	• 11832255E+00
1	5	4	• 12447254E+00	• 12447254E+00	• 12447254E+00	• 12447254E+00
2	5	4	• 17132158E+00	• 17132158E+00	• 17132158E+00	• 17132158E+00
3	5	4	• 18201935E+00	• 18201935E+00	• 18201935E+00	• 18201935E+00
4	5	4	• 18138835E+00	• 18138835E+00	• 18138835E+00	• 18138835E+00
5	5	4	• 17465515E+00	• 17465515E+00	• 17465515E+00	• 17465515E+00
6	5	4	• 17216181E+00	• 17216181E+00	• 17216181E+00	• 17216181E+00
7	5	4	• 17361725E+00	• 17361725E+00	• 17361725E+00	• 17361725E+00
8	5	4	• 17716568E+00	• 17716568E+00	• 17716568E+00	• 17716568E+00
9	5	4	• 18181913E+00	• 18181913E+00	• 18181913E+00	• 18181913E+00
10	5	4	• 18365668E+00	• 18365668E+00	• 18365668E+00	• 18365668E+00
11	5	4	• 18271566E+00	• 18271566E+00	• 18271566E+00	• 18271566E+00
12	5	4	• 17999999E+00	• 17999999E+00	• 17999999E+00	• 17999999E+00
13	5	4	• 17728014E+00	• 17728014E+00	• 17728014E+00	• 17728014E+00
14	5	4	• 17618434E+00	• 17618434E+00	• 17618434E+00	• 17618434E+00
15	5	4	• 17624655E+00	• 17624655E+00	• 17624655E+00	• 17624655E+00
1	5	5	• 13472143E+00	• 13472143E+00	• 13472143E+00	• 13472143E+00
2	5	5	• 23613441E+00	• 23613441E+00	• 23613441E+00	• 23613441E+00
3	5	5	• 24509441E+00	• 24509441E+00	• 24509441E+00	• 24509441E+00
4	5	5	• 27571755E+00	• 27571755E+00	• 27571755E+00	• 27571755E+00
5	5	5	• 20917502E+00	• 20917502E+00	• 20917502E+00	• 20917502E+00
6	5	5	• 21838546E+00	• 21838546E+00	• 21838546E+00	• 21838546E+00
7	5	5	• 22464772E+00	• 22464772E+00	• 22464772E+00	• 22464772E+00
8	5	5	• 24874621E+00	• 24874621E+00	• 24874621E+00	• 24874621E+00
9	5	5	• 26118854E+00	• 26118854E+00	• 26118854E+00	• 26118854E+00
10	5	5	• 27232255E+00	• 27232255E+00	• 27232255E+00	• 27232255E+00
11	5	5	• 28239781E+00	• 28239781E+00	• 28239781E+00	• 28239781E+00
12	5	5	• 29150745E+00	• 29150745E+00	• 29150745E+00	• 29150745E+00
13	5	5	• 40016153E+00	• 40016153E+00	• 40016153E+00	• 40016153E+00
14	5	5	• 41787895E+00	• 41787895E+00	• 41787895E+00	• 41787895E+00
15	5	5	• 41515154E+00	• 41515154E+00	• 41515154E+00	• 41515154E+00



2. Clamped square plate with concentrated centre load.







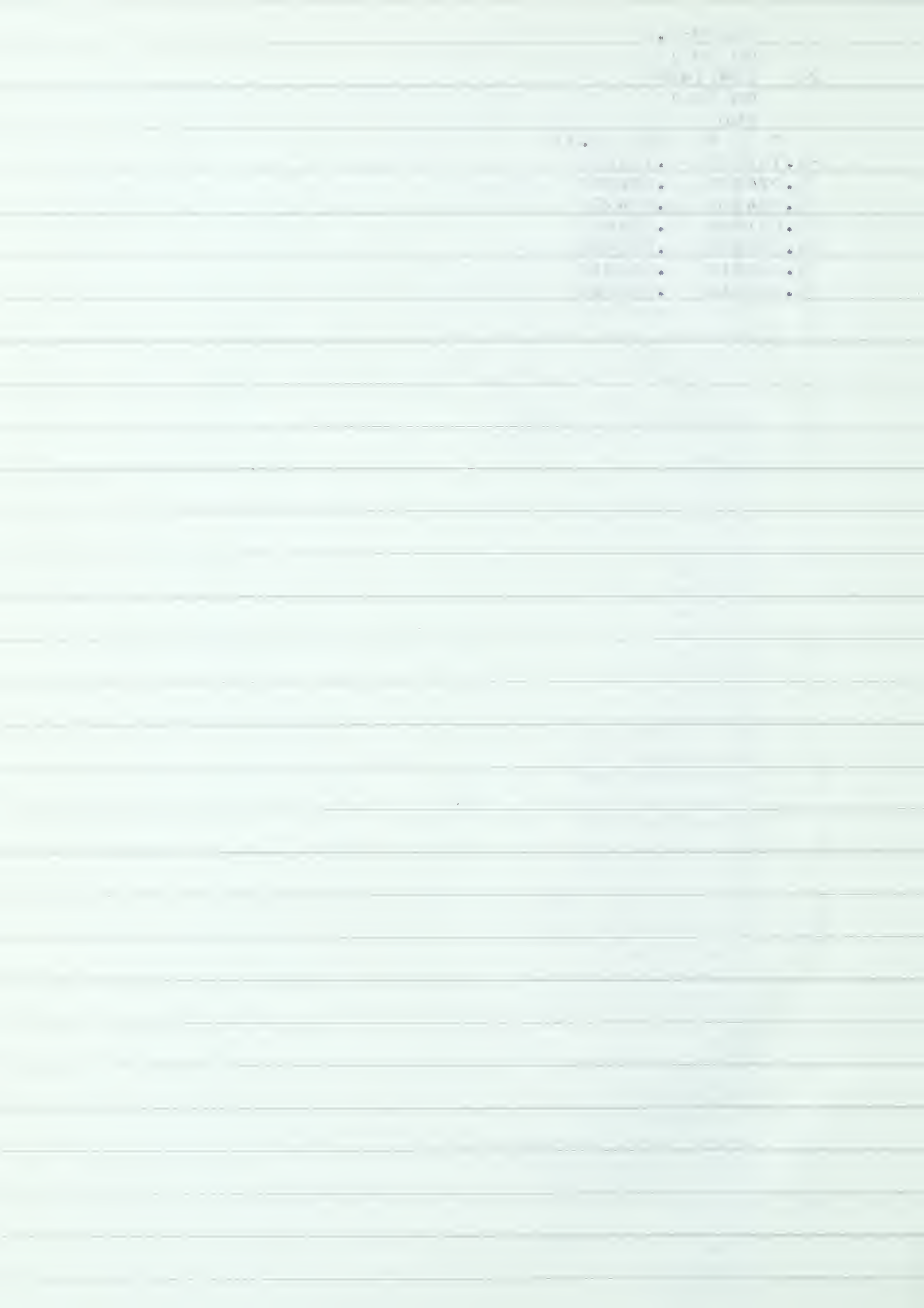
```

H=0.0 - INH=0.0 + H + H
THXX=2.0 *CC H+H H+H *C*H
CH=IANHM*COOH
THYY2=IAI-2.0*CHi+v H + INH + OCH
CHi=2.0 *COOH*COOH - H+H
H=IANHM*INH
THAT1=ICACDINH - INH + INH + INH
HAT2=INH + OCH = H + H
OCHX=PMI*COOHX
SHX=HT*INHX
THA13=INH+OCH=H
AA(MM)=CO L*(H - v*H - 2),CM
RA(MM)=AM*COOL*(H - v*H)
CA(MM)=RM*COOK*(H - v*H)
AI(MM)=COOL*(H - v*H - 2),CM
RI(MM)=AM*COOL*(H - v*H)
CI(MM)=RM*COOK*(H - v*H)
AA(.MM)=INL*(H - 1),CM
RAY(MM)=AM*INL*(H - 2)
SAX(.MM)=B*(H - INL*(H - 3)
UAM=0.0
U1M=0.0
SUXYM=0.0
IM=1
15
SA=0.0
SB=0.0
SC=0.0
SAY=0.0
SBi=0.0
SCi=0.0
AAi=0.0
RAi=0.0
CAY=0.0
DO 3 MM=1,IM
SAX=SAX+AX(MM)
SRA=SRA+RA(MM)
CA=CA+CI(MM)
AA=AA+AI(MM)
SBi=SBi+BI(MM)
SCi=SCi+CI(MM)
SAAT=SAAT+AY(MM)
SBAI=SBAI+BI(MM)
SCAY=SCAY+AY(MM)
P=1.0/3.14159
SUM=P*AA+RA+CA
SUYM=P*AI+BI+CI
SUXYM=P*SAY+SRAI+CAI
G=0.5
GU=(1.0-U)*0.5
UAM=G*SUM
TYM=G*SUYM
TAIM=GU*SUM
PUNCH 6,IM,L,K,MM,MM,MM
6 FORMAT(3I5,3E20.8)
IF(IM-1)14,20,20
IM=IM+1
TXM=0.0
TYM=0.0
SUXM=0.0
UYM=0.0

```



20 GO TO 15  
 20 CONTINUE  
 20 GO TO 1  
 20 END  
 7 5 5 1.53  
 -0.125 - 0.125  
 0.126300 0.2040  
 0.142 0.420  
 0.011500 0.17  
 0.010550 0.055  
 0.00021 0.0021  
 0.00060 0.006



••I M ECH. ENG. H-7 1231144  
••LOAD FORGO CLOCK 12 3

IM L K 1AM

TRIM

1AM

IM	L	K	1AM	TRIM	1AM
1	1	1	•11327420	•1564131	
2	1	1	•18356728	•2363861	
3	1	1	•2241871	•287278	
4	1	1	•25564816	•32816518	
5	1	1	•27915773	•3324847	
6	1	1	•29841101	•35172912	
7	1	1	•31462379	•3687118	
1	2	1	•99162700E-01	•15791118	
2	2	1	•1261604	•17658462	
3	2	1	•1978953	•1541329	
4	2	1	•81852855F-01	•13247434	
5	2	1	•60122550F-01	•11074512	
6	2	1	•52759440F-01	•133212	
7	2	1	•58991581F-1	•1961216	
1	3	1	•5766235F-1	•165297	
2	3	1	•79564171F-1	•53544285E-1	
3	3	1	-•2212106F-1	•2374827E-1	
4	3	1	-•6245710F-1	•4511041E-1	
5	3	1	•16168F-1	•6177712	
6	3	1	•231878F-1	•4814296E-1	
7	3	1	-•21142971E-2	•3662927E-1	
1	4	1	-•987133F-2	•4166251E-1	
2	4	1	-•795614F-1	-•1249681E-1	
3	4	1	-•29732040F-01	•4307447E-2	
4	4	1	-•51312450F-01	-•2317455F-2	
5	4	1	-•616115F-1	-•127644E-1	
6	4	1	-•42536460F-01	•645445E-2	
7	4	1	-•575724E-1	-•84779E-2	
1	5	1	-•12511	-•3382431E-1	
2	5	1	-•124826	-•42F41F-1	
3	5	1	-•1246118	-•411104E-1	
4	5	1	-•125120	-•4151314E-1	
5	5	1	-•12555019	-•4143143F-1	
6	5	1	-•125725	-•4148294F-1	
7	5	1	-•1257719	-•4148294F-1	
1	2	2	•6138233	•256271F-1	-•1091115-
2	2	2	•74161340E-1	•62F2585F-1	-•238706-
3	2	2	•6963215F-1	•62428715F-1	-•22268418-
4	2	2	•65368620F-01	•61187105E-1	-•320111-
5	2	2	•63505707F-01	•62681761F-1	-•28275A11
6	2	2	•6329465E-01	•6377721E-1	-•23112835-
7	2	2	•63422460F-01	•63737099F-1	-•20172322-
1	3	2	•313255F-1	•735647F-1	-•17173-
2	3	2	•64828305F-02	•2982562F-1	-•1044746-
3	3	2	-•18846410F-02	•21725615E-01	-•2443844-
4	3	2	•13731460F-02	•2922170E-01	-•253826-
5	3	2	•272341E-02	•2884773F-1	-•24425-
6	3	2	•214816F-02	•2954747E-1	-•241844-
7	3	2	•18988490F-02	•2016460F-1	-•24616311-
1	4	2	-•21641750F-01	•4024495E-1	-•2184544-
2	4	2	-•54166620F-01	-•56163E-2	-•11146-
3	4	2	-•43298110F-1	-•53876F-2	-•140221-
4	4	2	-•4556780F-01	-•43345F-1	-•20284-
5	4	2	-•478427F-1	-•545877F-2	-•16143-
6	4	2	-•422611F-1	-•56115E-1	-•1515-
7	4	2	-•435111E-1	-•44511E-1	-•114444-
1	5	2	-•746577E-1	-•5121784F-1	-•2850071-



2	2	-	• 4 6/4	-	• 141 15 7/7 -	-	• 1 4 1 -
3	2	-	• 1 636 65	-	• 1 1 1 1 -	-	• 1 4 1 -
4	5	-	• 1 4 1 2 284	-	• 44 44 44 44 -	-	• 1 4 1 2 2 -
5	2	-	• 1 4 1 4 1 4 8	-	• 141 1 1 1 1 -	-	• 1 4 1 2 2 1
6	5	2	-	• 1 4 1 6 2	• 141 1 4 1 4 1 -	-	• 1 3 8 3 1 4
7	5	1	-	• 1 7 3 4 2 0 5	• 141 1 8 1 2 2 -	-	• 1 7 3 4 2 1 5
1	3	3	-	• 727320351 - 12	• 54142 1 1 1 -	-	• 24111 1 1 1 -
2	2	1	-	• 5 6 5 7 1 F - 1	• 227 5 2 5 -	-	• 1 4 1 5 7 1 -
3	2	3	-	• 2 3 3 4 1 9 2 F - 1	• 1 1 1 8 4 2 5 -	-	• 1 4 1 6 2 1 -
4	2	3	-	• 2 6 1 5 2 6 4 7 F - 12	• 1938851 F - 2	-	• 1 4 1 6 5 1 -
5	3	3	-	• 1 9 3 3 7 1 1 F - 11	• 141 2 6 5 1 F - 2	-	• 1 4 1 6 5 1 -
6	3	3	-	• 1 9 6 5 4 2 F - 2	• 1 9 6 1 1 1 5 - 2	-	• 1 4 1 6 5 1 -
7	3	3	-	• 1 9 6 5 7 1 F - 2	• 1 9 6 1 1 1 5 - 2	-	• 1 4 1 6 5 1 -
1	4	3	-	• 2 5 1 0 9 9 2 4 F - 11	• 14651 1 1 4 1 -	-	• 2 5 8 1 4 1 1 F -
2	4	3	-	• 3 2 2 7 3 2 8 7 F - 1	• 2 1 4 2 6 5 F - 2	-	• 2 6 1 8 2 1 10 -
3	4	3	-	• 2 9 9 9 7 1 1 F - 1	• 1 2 1 4 2 1 6 F - 1	-	• 2 2 1 1 6 1 4
4	4	3	-	• 3 1 7 5 7 1 1 F - 1	• 1 2 1 2 4 3 5 F - 1	-	• 2 2 4 3 6 7 1 F -
5	4	3	-	• 3 2 1 1 3 2 1 F - 11	• 1 1 6 2 6 1 F -	-	• 2 2 8 1 8 4 6 1
6	4	2	-	• 3 2 2 3 5 3 F - 1	• 1 1 8 1 4 F -	-	• 2 2 8 1 8 4 6 1
7	4	3	-	• 3 2 3 1 8 2 F - 1	• 1 1 8 2 5 1 -	-	• 2 2 8 1 8 4 6 1
1	5	3	-	• 7 2 4 7 9 5 4 0 F - 11	• 2 2 1 7 9 7 4 F - 1	-	• 2 4 1 1 4 2 3 -
2	5	2	-	• 5 2 5 1 5 6 F - 1	• 2 2 1 7 9 7 4 F - 1	-	• 2 4 1 1 4 2 3 -
3	5	3	-	• 5 6 8 5 1 4 4 F - 1	• 1 1 6 1 4 1 -	-	• 1 1 6 1 4 1 -
4	5	3	-	• 5 7 1 2 1 1 0 F - 1	• 1 2 1 1 7 6 1 F - 1	-	• 1 1 4 2 1 4 1 -
5	5	3	-	• 5 7 2 1 1 1 F -	• 1 2 1 2 2 2 F - 1	-	• 1 2 1 2 1 2 1 -
6	5	3	-	• 7 7 3 1 4 7 1 F - 1	• 2 2 1 3 8 2 3 F -	-	• 1 2 1 2 1 2 1 -
7	5	2	-	• 5 4 1 7 1 4 4 F - 1	• 2 2 1 4 1 5 4 F -	-	• 1 2 1 2 1 2 1 -
1	4	4	-	• 2 1 4 0 7 9 8 1 - 1	• 2 6 1 1 4 1 F -	-	• 1 8 1 8 4 1 8 6 1 -
2	4	4	-	• 1 5 1 2 4 7 4 0 F - 1	• 1 4 2 1 1 1 1 F -	-	• 1 2 1 2 1 2 1 -
3	4	4	-	• 1 4 8 4 6 1 5 F - 11	• 1 4 1 1 4 1 1 F -	-	• 1 2 1 2 1 2 1 -
4	4	4	-	• 1 4 8 4 2 9 6 0 F - 1	• 1 4 8 4 5 0 2 F -	-	• 1 5 2 1 0 2 1 -
5	4	4	-	• 1 4 8 4 7 1 7 F - 11	• 1 4 2 4 1 3 5 F -	-	• 1 6 3 1 4 1 -
6	4	4	-	• 1 4 8 6 1 6 F - 1	• 1 4 1 3 2 6 5 F -	-	• 1 6 3 1 4 1 -
7	4	4	-	• 1 4 8 5 1 7 5 4 F - 1	• 1 4 8 4 6 1 4 F -	-	• 1 5 1 3 4 -
1	5	4	-	• 3 9 2 2 1 2 1 - 1	• 1 2 1 4 4 2 4 F -	-	• 2 4 1 2 1 8 7
2	5	4	-	• 1 4 1 2 6 2 8 6 F - 1	• 4 2 2 9 1 1 1 - 2	-	• 1 4 1 2 1 4 -
3	5	4	-	• 1 1 4 6 6 6 1 F -	• 1 5 4 4 2 1 F -	-	• 1 4 1 2 1 4 -
4	5	4	-	• 1 4 7 2 6 1 7 F - 1	• 1 4 7 1 1 8 1 F -	-	• 1 4 1 2 1 4 -
5	5	4	-	• 1 6 8 1 1 8 F - 11	• 1 4 2 4 1 5 4 F -	-	• 1 5 1 3 4 -
6	5	4	-	• 1 8 1 7 1 3 0 F -	• 1 4 2 4 1 4 4 F -	-	• 1 5 1 3 4 -
7	5	4	-	• 1 9 3 2 1 0 3 F - 1	• 2 5 1 1 1 2 1 F - 2	-	• 1 3 1 2 -
1	5	5	-	• 4 2 8 1 1 5 1 3 E - 11	• 4 1 8 1 5 4 F -	-	• 1 0 1 4 1 5 -
2	5	5	-	• 5 9 1 1 9 3 4 0 F - 18	• 5 7 1 1 0 5 5 F -	-	• 4 2 1 4 1 5 2 -
3	5	5	-	• 7 1 5 1 4 6 4 4 F - 18	• 1 8 1 8 1 1 1 F -	-	• 1 0 1 6 4 1 4 -
4	5	5	-	• 8 3 3 4 1 5 F - 18	• 8 4 1 2 4 F -	-	• 1 4 1 2 1 4 -
5	5	5	-	• 1 6 5 2 0 3 2 F - 7	• 1 2 3 4 3 1 7 1 F -	-	• 1 4 1 2 1 4 -
6	5	5	-	• 1 7 5 6 2 1 2 2 F -	• 1 4 2 1 1 4 F -	-	• 1 4 1 2 1 4 -
7	5	5	-	• 1 7 9 5 8 6 6 F - 1	• 1 7 1 1 3 3 0 F -	-	• 2 1 1 1 1 1 1 F -



BIBLIOGRAPHY

1. P. K. Ligtenberg, "The Moiré Method - new experimental method for the determination of Moments in Small Slab Models," Proceedings of the Society for Experimental Stress Analysis Vol. 2, No. 2, 1954.
2. W. A. Bradley, "The Determination of Moments and deflections in Plates by the Moiré Method and by Finite Difference with Application to The Square Clamped Plate with Square Cutouts," Doctoral Thesis, University of Michigan, 1956.
3. W. A. Bradley, "Laterally Loaded Thin Flat Plates," Proceedings of A.S.C.E. (EM) Vol. 85, 1959, P.77.
4. P. J. Palmer, "Bending Stresses in Cantilever Plates by Moiré Fringes," Aircraft Eng. Vol. 29 no. 346, December, 1957, P.377-80.
5. B. B. Raju, "A Study of Simply Supported Square Plates by the Moiré Method and by Finite Difference," Master's Thesis, Michigan State University, 1958.
6. S. Timoshenko, "Theory of Plates and Shells," McGraw-Hill Book Co., New York, 1959.
7. D. Young, "Clamped Rectangular Plates with a Central Concentrated Load," Trans. A.S.M.E. Vol. 61, 1939.
8. A. Nadai, "Discussion of Clamped Rectangular Plates with a Central Concentrated Load," J. of App. Mech. Vol. 62, March, 1940, P.A-41.
9. R. G. Sturm, and R. L. Moore, "The Behavior of Rectangular Plates Under Concentrated Load," J. of App. Mech. Vol. 4-no. 2, June, 1937, P.A-75.
10. D. L. Holl, "Cantilever Plate with Concentrated Edge Load," Trans. A.S.M.E. Vol. 59, 1937, P.A-8.
11. R. Weller and B.M. Shepard, "Displacement Measurement by Mechanical Interferometry," Proc. S.E.S.A. no. 1, 1948.
12. S. Morse, A. J. Durelli, C. A. Sciammarella, "Geometry of Moiré fringes in Strain Analysis," Proc. A. S. C. E. Vol. 86 no. EM 4, August, 1960, pt. 1, paper no. 2576, p. 105-26.



13. I. A. B. Low, and J. W. Bray, "Strain Analysis Using Moiré Fringes," *Engineer*, 1962, p. 567.
14. W. F. Riley, A. J. Durelli, "Application of Moiré Methods to the Determination of Transient Stress and Strain Distributions," *J. of App. Mech.* March, 1962, p. 23.
15. C. G. J. Vreedenburgh and H. Van Wijngaarden, "New Progress in our Knowledge about the Moment Distribution in Flat Slabs by Means of the Moiré Method," *Proceedings of the Society for Experimental Stress Analysis* Vol. 2 no. 2, 1954.













**B29813**